Examensarbete
TVVR 11/5007

Wave atlas along the south-eastern coast of Sweden

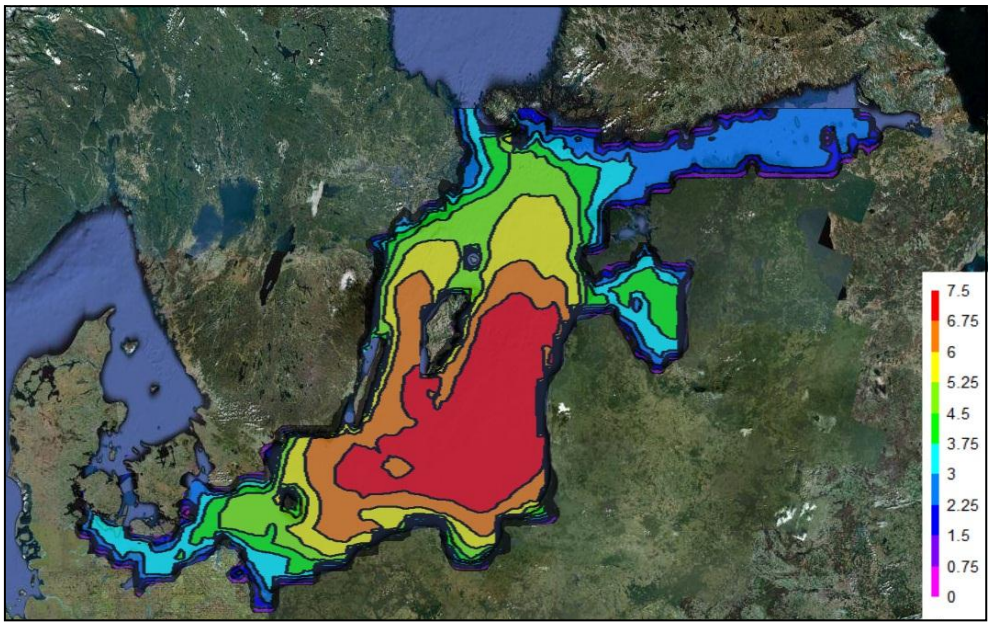

A 6-year simulation of waves using local wind measurements from meteorological stations around the Baltic Sea.

Sebastian Irminger Street

Division of Water Resources Engineering
Department of Building and Environmental Technology
Lund University

Avdelningen för Teknisk
Vattenresurslära
TVVR-11/5007
ISSN-1101-9824

Wave atlas along the south-eastern coast of Sweden

A 6-year simulation of waves using local wind measurements from meteorological stations around the Baltic Sea.

Key words: Baltic Sea, wave modelling, WAM, forcing through wind measurements, wave climate

Sebastian Irminger Street

Acknowledgments

I would like to thank Marcus Flarup of the SMHI, Thomas Bruns of the DWD and Heidi Pettersson and Asko Huttila of the FMI for their kind and patient help in supplying me with wind and wave data measurements, along with Pham Thanh Nam for all his efforts in helping me understand the Fortran programming language. I am also deeply grateful to Luciana Bertotti of the Institute of Marine Science in Venice for teaching me how to use the WAM model and constantly supplying me with support when I ran into problems. Last but not least I would like to thank my supervisors from Lund university, Hans Hanson and Magnus Larson, for always being available when I needed second opinions.

Abstract

A wave atlas describing the monthly wave climate at 5 locations along the Swedish SE coast was desired. Using the WAM wave model to hindcast the waves between Jan 1st 2004 and Dec 31st 2009 the parameters *significant wave height*, *direction of wave propagation* and *spectral wave peak period* were extracted from the time series and assembled in a wave atlas. The model was forced with point source wind measurements from meteorological stations in coastal areas around the southern Baltic Sea. To accommodate for differences in winds on land and over water the wind measurements were compensated through a logarithmic expression deriving from experiments at the American Great Lakes. Validation of the model results against buoy measurements showed that the chosen approach was able to reproduce the general trends of the wave climate, even if single events could be misrepresented. The larger wave heights were generally underestimated.

The resulting wave atlas showed April-Aug as a calmer period with average H_S 0.7-1 m while Nov- Feb was a period of higher waves with average H_S 1-1.5 m. Waves for rough conditions, determined as the average of the top 10% of H_S for every month, were in the range 1.2-2 m and 2-2.7 m for the respective periods, while the maximum values were in the range of 2-4 m and 2.9-4.6 m, respectively. The high waves during the calmer period were due to reoccurring storms in June around the southern tip of Sweden.

Wave propagations, determined as the direction in which the waves travelled, were mainly in the range N/NE/E from June-Dec. During the late winter and early spring there was an increase in westerly waves, culminating around March/April.

Model results of wave peak periods were difficult to interpret due to large scatter. The average monthly peak period showed only minor annual variations, with values for all months being between 4-6 seconds. Maximum peak periods varied a little more, between 7.5-11 seconds. Through visual comparison of measurement values and model results the average values of T_p are considered trustworthy, but the large scatter of the results make the maximum values of T_p less certain

The resulting wave atlas is primarily intended for practical applications and as guidelines for design in and around the 5 selected locations. The results can also be used as input to more detailed computer models of the surf zone.

Table of Contents

1 Introduction

1.1 Background

For as long as there has been naval commerce, vessels have needed shelter from waves while loading or unloading their cargo. Smaller vessels found shelter in natural bays, but as ships and cargo loads grew so did the need for permanent sheltering structures. Protection against waves therefore gave birth to a new discipline of engineering, coastal engineering. Modern coastal engineering embraces much more than just harbour construction, but waves remain a crucial component of any coastal intervention. Understanding the wave characteristics of an area is therefore necessary in most coastal work.

To describe an area's wave characteristics, statistical analyses can be carried out on long-term wave observation series. Such analyses will result in a wave atlas, giving representative values of the waves that can be expected in the area. An inherent limitation of such an approach, however, is the difficulty in finding locations with long enough or reliable enough data series.

When lacking actual observations a computer model can be used to describe waves over long periods of time. Using these results the same statistical analyses can be run to produce a wave atlas for an area.

1.2 Waves in the Baltic Sea

The Baltic Sea is a semi-enclosed water body covering an area of 448 000 km^2 and holds a water volume of 27 500 km^3 (SMHI, 2009a). The Baltic Sea is relatively shallow, with average depth of only 55 m, but at its deepest it reaches 450 m (Östersjöportalen, 2011). The Baltic Sea can be sub-divided into the Sea of Bothnia to the north and the southern Baltic Sea to the south. The coverage of the two is 61 000 km^2 and 387 000 km^2 respectively (SMHI, 2009a).

The highest individual recorded wave in the Baltic Sea was 14 m high, and was measured south of Åland on Dec 22nd 2004 (SMHI, 2010). The significant wave height at the time was 7.7 m. Such high waves are rare in the Baltic as the enclosed nature of the basin means that all wave generation must take place within the basin itself, and is therefore limited by the fetch of the basin. In the Baltic Sea the longest fetches are approximately 800 km. The average values of the significant wave heights, calculated from available buoy measurements, for three locations in the Baltic Sea can be seen in Figure 1.

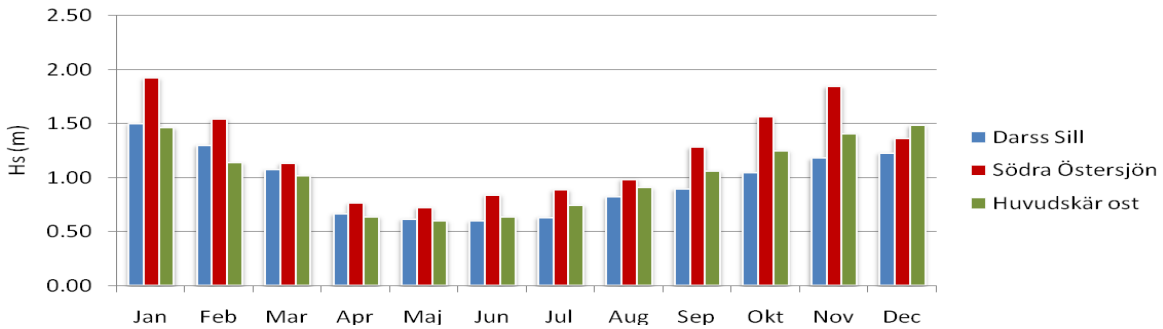

Figure 1 *Average monthly significant wave heights for three locations in the Baltic Sea. The values are based on available buoy measurements*

1.3 Objectives, scope and limitations

This study has two main objectives. The first one is to assess the effects of forcing the WAM wave model with point source wind measurements from meteorological stations in coastal areas instead of, as customary, using wind fields generated by meteorological models. Each station will be assigned an area of influence over which the station's measurement is assumed to be valid, and by combining the areas a wind field over the Baltic will be created. This approach has been used by *e.g.* Blomgren, *et al.* (2001) with acceptable results. The reasons for choosing point-source measurements rather than the conventional approach are several.

1. It is of scientific interest to know how the model reacts to point measurements.
2. In practical applications one does not always have access to wind fields generated by meteorological models.
3. Like all models, meteorological models have their weaknesses. By using actual measurements assumptions and simplifications used by the meteorological models can be avoided.

Some of the downsides of using point measurements are;

1. The measurements are extremely local and stand high risk of being influenced by surrounding topography and/or buildings. Local disturbances will then be transferred onto the entire area of influence.
2. A representative way of merging measurements from different stations into one wind field must be found. This can prove difficult if several weather systems are affecting the modelled area at the same time.

Model performance will be evaluated with respect to significant wave height, peak period and direction of wave propagation. If an acceptable model performance is achieved when forced by point source measurements a second objective will be introduced. Using winds between 2004 and 2009 the medium-term wave climate at Falsterbo, Ystad, Hanöbukten, the southern tip of Öland and south of Nynäshamn will be established. The locations chosen can be seen in Figure 2, along with latitudes, longitudes and the water depths used by the model at the locations.

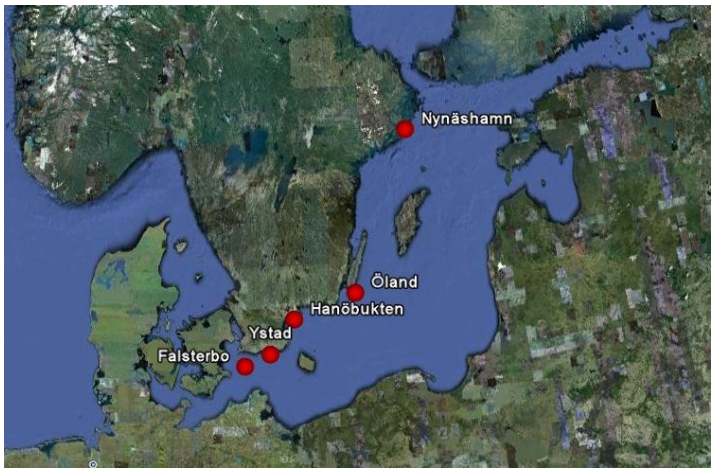

Location	Lat	Lon	Depth
Falsterbo	55.11	13.02	29
Ystad	55.31	13.82	14
Hanöbukten	55.91	14.62	9
Öland	56.31	16.62	11
Nynäshamn	59.11	18.82	11

Figure 2 *Locations at which a wave atlas will be determined.*

The study will only consider waves within the Baltic Sea, so Skagerrak and Kattegat will be excluded from the studied area. As the study's final aim is the description of waves in the southern Baltic Sea the Sea of Bothnia will be excluded, if such an exclusion can be shown not to affect the waves in the south.

2 Introduction to numerical modelling

Numerical modelling of any kind is a way of describing the physical world around us in mathematical terms. When it comes to wave modelling this could *e.g.* mean finding the wave height (=deviation of the water surface from a mean level), the energy transmitted by a wave or the direction in which the wave propagates. The physical understanding of how a moving wind exerts a drag force on a water surface allows the modeler to mathematically reconstruct the effects of an actual wind blowing over a free water surface.

In order to create a model the modeler must first step away from the real world of continuums and view the world as being discretized. Spatial discretization will often be a first step, in which the modeler assumes that the modeled area can be sub-dived into a finite number of cells of predefined size (as opposed to the reality of an infinite amount of infinitely small cells). By dividing an area like this a model grid is obtained, with a grid resolution corresponding to the cell size. The second step will be a temporal discretization in which the modeler selects a period of time over which all parameters will be considered constant. This time step is referred to as the calculation time step. By discretizing the continuums of both time and space the modeler has gained a way of representing the effect of wind at every grid point and at every time step, enabling descriptions over large areas and over long periods of time.

Numerical wave modelling saw its first boom during the Second World War, when wave forecasts were desired for military planning purposes (Jensen, 1994). In the 40's and 50's ways were found to relate wind speed/wind duration/fetch to wave height by formulation of the *significant wave height method* (see *e.g.* (Sverdrup&Munk, 1947) or (CEM, 2006)), meaning that the sea-state was approximated by one single representative value. Such lumping of wave characteristics was crude, but lacking the computational possibilities of today it offered an accessible way of describing the main characteristics of the sea-state. As time went by both the computational capacities available and our physical understanding of wind-wave and wave-wave interactions increased and a spectral approach to wave modelling was adopted.

2.1 Spectral wave modelling

A spectral approach implies that the sea-state is no longer considered the result of one single wave, but rather as the sum of many different waves (Rosman, 2007). The benefit of such a concept is that a seemingly random sea-surface can be described by a number of regular sinusoidal waves, according to Figure 3.

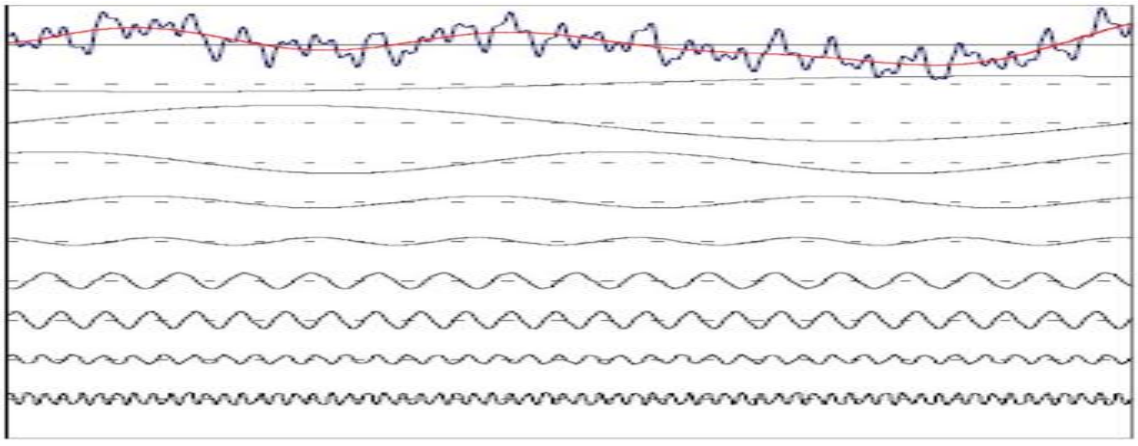

Figure 3 *Description of how a seemingly random sea-state (top line) is really the sum of a number of regular sinusoidal signals (Rosman, 2007).*

Each sinusoidal wave will have its own amplitude and frequency and the sum of all waves will be the resulting sea-state. The energy contained within each wave can be calculated from its frequency and then plotted to show how the total energy of the sea-state is distributed over the frequencies. This is called a 1-D energy spectrum with respect to frequency, and an example of this can be seen in Figure 4.

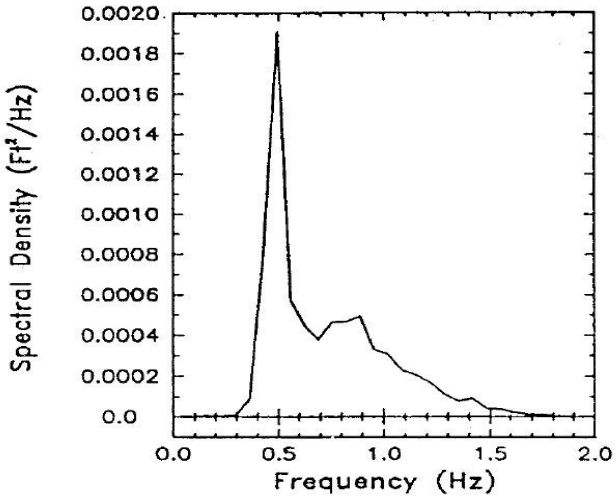

Figure 4 *Example of a 1-D energy spectrum with respect to frequency. (CEM, 2006)*

So far only the variation of the energy density with respect to wave frequency has been discussed, but as energy is transported by waves the direction of wave propagation must also be of importance to the distribution of energy. Waves are free to travel in any horizontal direction, so the energy density must be a function of both the wave frequency and the direction of propagation. How the WAM model deals with this will be discussed in Chapter 2.2, but an example of what the results may look like can be seen in Figure 5. By analysing the 2-D energy spectra the modeller can learn not only which frequency holds the most energy, but also which direction the bulk of the energy is travelling in.

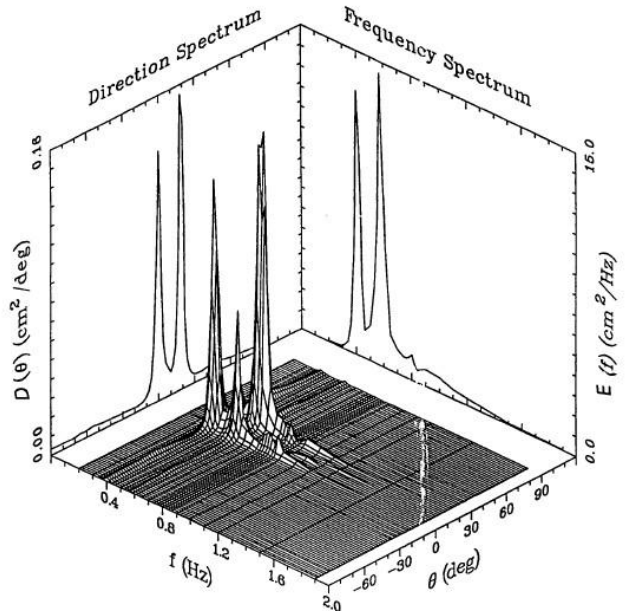

Figure 5 *Example of 2-D energy spectrum with respect to frequency and direction of propagation. (CEM, 2006)*

2.2 The WAM model

The WAM model is a so called 3rd generation wave model. No in-depth description of the differences between 1st, 2nd and 3rd generation models will be given here, for detailed descriptions see *e.g.* (Komen, *et al.*, 1994) or (Jensen, 1994). Suffice is to say that earlier generations were hampered in their modelling of wave-wave interaction by either neglecting it or requiring a priori assumptions for the wave spectrum shape. This meant that model development became site specific and non-universal. In 3rd generation models the spectrum is free to take any shape and is therefore universal.

As mentioned earlier the distribution of energy density for a wave field will depend on both the wave frequency and the direction of propagation. For WAM to handle this the directional and frequency spectrums must be discretized by the user, stating the number of directional and frequency bins (=intervals) used in a run along with the lowest frequency the user wishes to use. By stating the lowest frequency used and the number of frequency bins the highest frequency is automatically obtained. By discretizing the directional and frequency spectrums the WAM model can produce a 2D energy density spectrum at each model grid point and time. The energy density spectrum is represented by an NxM matrix, in which N represents the directional bins and M the frequency bins. By adding the N values of energy density over each frequency bin the energy density spectrum with respect to frequency can be created. Figure 6 shows the creation of the energy density spectrum from an imaginary 5x5 matrix. The same logic can also be applied to create the energy density spectrum with respect to direction.

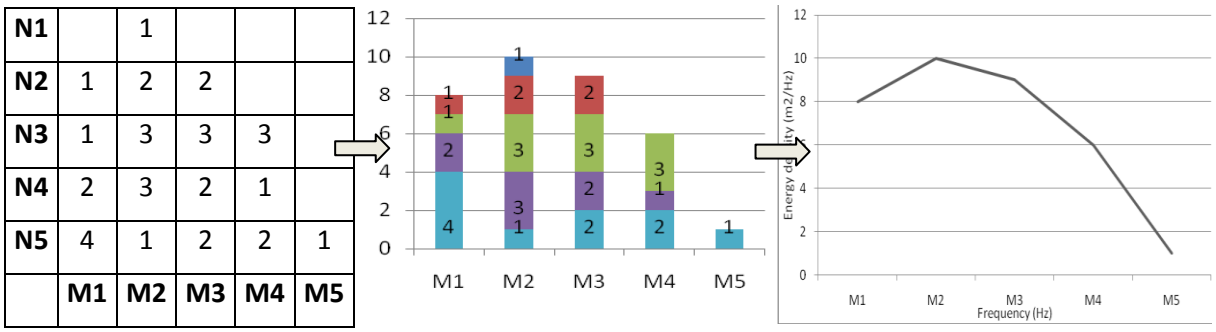

Figure 6 *Creation of energy spectrum with respect to frequency. The values above each M column are added up to form the spectrum.*

The baseline mathematics used in WAM is an energy balance known as the transport equation (TE). The TE shows how energy shifts within a system by stating that the change of energy is equal to the sum of all source and sink terms subtracted by the energy leaving the system as waves crossing the system boundary. The transport equation is written as

$$\frac{\partial E}{\partial t} + \overrightarrow{c_g} \cdot \vec{\nabla} E = \sum S_i$$

- E is the two-dimensional energy density spectrum with respect to wave frequency and direction of propagation at each grid point and time.
- c_g is the group wave velocity.
- S_i is the combined source or sink terms adding or taking energy to/from the system.

For the WAM model the source and sink terms include are

1. S_w- input of energy through wind-wave action. The input comes from the drag the wind exercises on the water surface and is the only energy input to the system.
2. S_{ds}- loss of energy through dissipation and through white-capping or breaking of waves.

3. S_{nl}- non-linear redistribution of energy within the spectrum due to wave-wave interaction. Energy will be moved from higher frequencies to the lower ones causing a lowering of the peak frequency and a pointier energy spectrum as time goes by, shown in Figure 7.

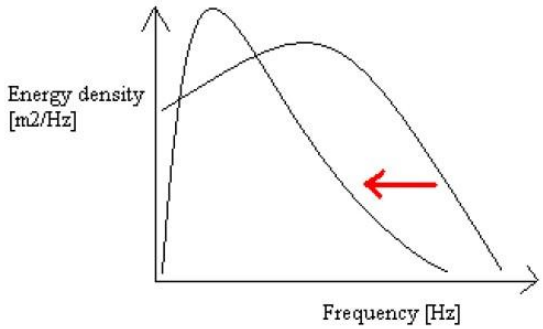

Figure 7 *Energy being shifted from high frequencies to low frequencies due to wave-wave interaction.(Berg, n.d.)*

4. S_{bf}- sink term showing energy loss due to bottom friction and percolation. Only relevant when modelling in shallow water.

2.3 The model setup of the study

For this study the model was run in shallow water mode and refraction was included. The properties of the directional and frequency bins are summarized in Table 1.

Table 1 *Properties of the directional and frequency bins.*

Number of directional bins	24
Span of each directional bin	15^{o}
Number of frequency bins	30
Lowest frequency/period	0.05 Hz/20 sec

3 Description of available data in the study area

In order to function properly the WAM model required at least two indata files; the bathymetry of the modelled area and the wind field acting over the same. In addition to this currents and ice coverage can also be included.

Chapter 3 will only describe the properties of the indata used for this study. The necessary analysis and manipulation of the indata is left for Chapter 4.

3.1 Bathymetry

A high-resolution, spherical bathymetric grid of the Baltic Sea region was obtained from the Leibniz Institute for Baltic Research (IOW). The grid stretched from latitudes 53.30°-66.00° and longitudes from 9.00°-31.00° (degrees given as decimal degrees). The resolution of the grid was 2 minutes in longitude and 1 minute in latitude, equal to 1/30th and 1/60th of a degree. The full grid coverage can be seen in Figure 8.

Figure 8 *Area covered by the original 2x1 minute bathymetric grid*

3.2 Winds

Details on all the meteorological stations used in the study can be found in Appendix 1.

3.2.1 Winds from Sweden

From Sweden five meteorological stations (Falsterbo, Ölands södra udde, Hoburg, Gotska sandön and Svenska högarna) along the Swedish east coast were used. Winds were collected and supplied by the Swedish Meteorological and Hydrological Institute (SMHI) on a 3-hourly basis for the period 1961-2009, although not all stations have the full period coverage. The locations of the stations and their periods of measurements are illustrated by Figure 9 and Figure 10 in Chapter 3.6.

3.2.2 Winds from Germany
From Germany two meteorological stations (Arkona and Fehrman) located along the German north coast were used. The data was supplied by the Deutscher Wetterdienst (DWD) on a 3-hourly basis for the period 2004-2010. The locations of the stations and their periods of measurements are illustrated by Figure 9 and Figure 10 in Chapter 3.6.

3.2.3 Winds from Latvia
From Latvia three meteorological stations (Liepaja, Kolka and Pavilosta) located along the Latvian western coast were available. One of the stations, Pavilosta, was quickly deemed completely unreliable while the remaining two were deemed suspicious, as will be shown in Chapter 4.1.3. The data was supplied on a 3-hourly basis by the Latvian Environment, Geology and Meteorology Centre (LEGMC) for the period 2004-2009. The locations of the stations and their periods of measurements are illustrated in Figure 9 and Figure 10 in Chapter 3.6.

3.2.4 Winds from Finlad
From Finland two meteorological stations (Gråhara and Russarö) located in the Gulf of Finland were used. The data was supplied on a 3 hourly basis by the Finish Meteorological Institute (FMI) over the period 2004-2009. The locations of the stations and their periods of measurements are illustrated in Figure 9 and Figure 10 in Chapter 3.6.

3.3 Ice
The Baltic Sea is subjected to subfreezing temperatures during long parts of the year, and substantial areas of the Sea of Bothnia freeze every winter (SMHI, 2009b). Even if ice coverage has a massive impact on wave propagation, effectively acting as if it the wave hit land, ice data was not included in this study. This was primarily due to the facts that

- the area of main interest was the southern Baltic Sea, where freezing is less frequent (SMHI, 2009b).
- when using results from medium-term modelling for future planning it is highly relevant to see how the Baltic reacts to winds under ice-free conditions, as one can not always count on ice being present to protect against waves.

3.4 Currents
Currents have a small impact on the wave climate, and were not included in the study.

3.5 Waves
Details on all the wave buoys used in the study can be found in Appendix 1.

3.5.1 Wave data from Sweden
Wave measurements from six wave buoys were available from the SMHI, in total covering the period 1978-2010. Out of the six, three had coverage during 2004-2009. These were Södra Östersjön, Huvudskär ost and Finngrundet. The locations and periods of measurements of all the buoys are illustrated by Figure 9 and Figure 11 in Chapter 3.6. The available measurement parameters used in this study were the significant wave height (H_s), the direction of wave propagation and the peak period (T_p). Measurements were done as 10 min averages every hour.

3.5.2 Wave data from Germany
From Germany two wave buoys (Darss Sill and Arkona) were available from the DWD, covering the period 2004-2010. The locations of the buoys and periods of measurements are illustrated by Figure 9 and Figure 11 in Chapter 3.6. Unfortunately the only measurement parameter available from the German buoys was H_s.

3.5.3 Wave data from Finland

From Finland one wave buoy (Northern Baltic Proper) was available from the FMI, covering the period 2008-2009. The location of the buoy and its period of measurement is illustrated by Figure 9 and Figure 11 in Chapter 3.6. As the buoy did not cover the full period 2004-2009 this buoy was not used in the study.

3.5.4 Wave data from Latvia

No wave data was used from Latvia

3.6 Summary

- A high-resolution, 2x1 minute spherical bathymetric grid was supplied by the Leibniz Institute for Baltic Research.
- Wind measurements were obtained from 11 meteorological weather stations located in the coastal regions around the Baltic Sea. The location of the stations can be seen as green dots in Figure 9.
- Ice coverage and currents were excluded.
- Wave measurements from 6 wave buoys were obtained for the period 2004-2009, and a further 6 buoys for other periods. The buoys used can be seen as yellow dots in Figure 9, while other buoys are red.
- The periods over which wind and wave measurements were available can be seen in Figure 10 and Figure 11.

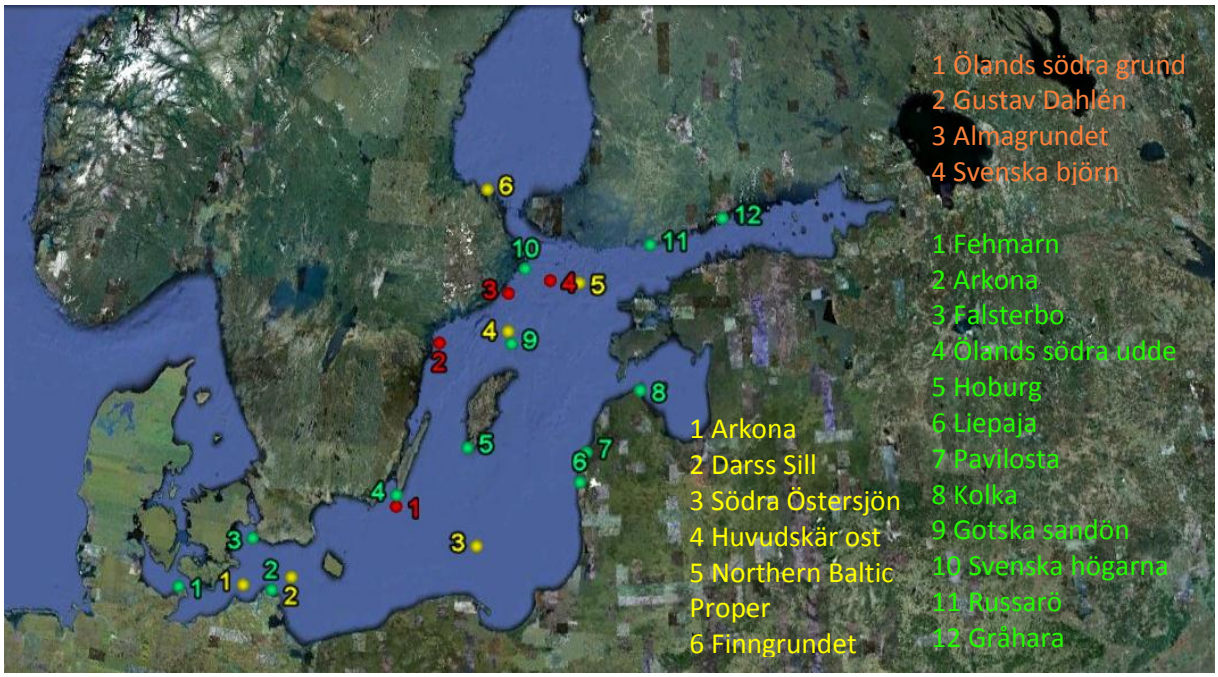

Figure 9 *Location of meteorological stations (green), wave buoys within the period 2004-2009 (yellow) and other wave buoys (red).*

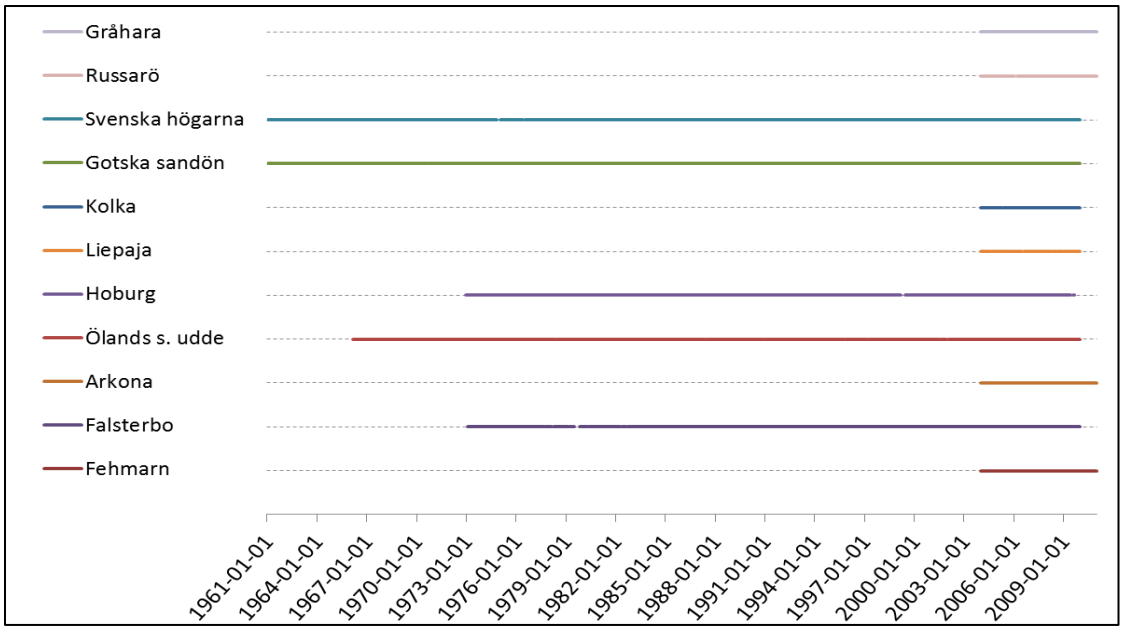

Figure 10 *Duration of available wind measurements.*

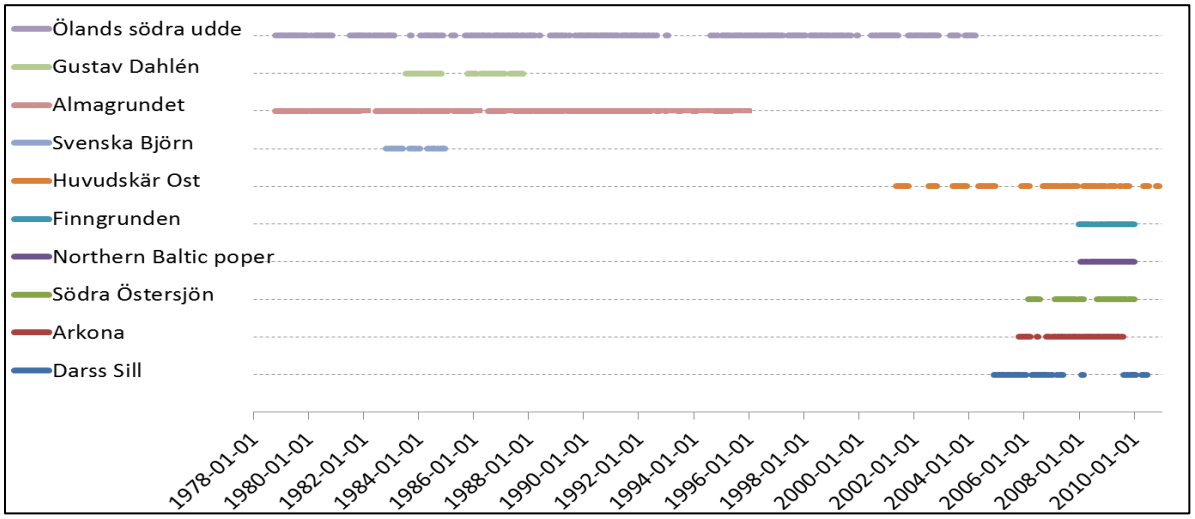

Figure 11 *Duration of available wave measurements.*

4 Analysis of available data

4.1 Analysis of wind measurements

4.1.1 Sweden

To assess if winds acting at the Swedish meteorological stations shared similar patterns the wind direction measurements were subdivided into 8 intervals. To facilitate the comparison between countries the graphic results for all four countries will be presented jointly in Figure 12 and Figure 13 in Chapter 4.1.5. The results showed that winds were prevailingly south-western at most of the stations. Svenska högarna experienced more northern winds than the others, but even so about 50% of all winds at all five stations were in the range S-SW-W, showing that the wind stations were generally affected by the same weather system.

Wind speeds between the stations were also compared for the period 1961-2009. A list of maximum, average and median wind speeds can be found in Table 2, along with the total amount of valid measurements used. The data showed that winds at all the Swedish stations presented similar characteristics, with a maximum speed of approximately 30 m/s (Ölands södra udde is extreme with 39 m/s) and an average of approximately 6.0-7.0 m/s. Svenska högarna, the most northern station, was a little bit windier with an average of 7.5 m/s. Combining the similar wind speeds with the similar wind directions it seems clear that all the Swedish met stations are generally affected by the same weather system.

Table 2 *Summary of wind speed characteristics at the SMHI meteorological stations for the period 1961-2010.*

Station name	Max. speed	Average speed	Median speed	Available measurements
Falsterbo	28	6.6	6	130 967
Ölands södra udde	39	7.0	7	137 540
Hoburg	30	6.2	6	122 448
Gotska sandön	30	6.1	6	141 951
Svenska högarna	30	7.5	7	141 670

4.1.2 Germany

Just like the Swedish case the German wind direction measurements were subdivided into 8 directions to assess whether winds acting along the German coast were affected by the same weather system. The results are presented in Chapter 4.1.5 and showed very similar wind patterns as those seen at Falsterbo, with mainly W and SW winds.

German wind speed measurements were supplied in unit knots, and were therefore converted as $1\ \text{knot} = 0.514\ \text{m/s}$. The characteristics then obtained are presented in Table 3. Maximum wind speeds were 2-3 m/s lower than the corresponding Swedish winds at Falsterbo, while the average wind speeds were very similar at approximately 6.5 m/s.

Table 3 *Summary of wind speed characteristics at the DWD meteorological stations for the period 2004-2010.*

Station name	Max. speed	Average speed	Median speed	Available measurements
Fehmarn	25.2	6.3	6.2	20 427
Arkona	26.3	6.6	6.4	20 407

4.1.3 Latvia

To assess whether winds acting along the Latvian coast were affected by the same weather system as the German and Swedish stations the wind direction measurements were subdivided into 8 directions. The results are presented in Chapter 4.1.5. It was seen that wind directions at Pavilosta differed substantially from those at Liepaja and Kolka with a clear “spike” towards SE. As Pavilosta is located between Kolka and Liepaja the great difference in wind directions can only be explained by local topography affecting the measurements at Pavilosta. Pavilosta

meteorological station was therefore not trusted to give representative values of the area surrounding it, and was excluded from the study. Liepaja and Kolka both showed directional patterns similar to those seen for Sweden.

The wind speed measurements from the three Latvian stations were also examined. The results are presented in Table 4. When compared to both Swedish and German measurements it was seen that Latvian wind speed measurements were low (average speed 2.8-3.6 m/s, max speed 13-19 m/s). This was surprising as the directional analysis showed that the same directional patterns affecting both Sweden and Latvia, leading to the conclusion that the same weather system is active over the entire Baltic region. Bearing this in mind there seems to be no reason as to why winds on the eastern half of the Baltic are lower than on the western half. On the contrary, as the wind is blowing over open water one would rather expect an increase in wind speed on the eastern side compared to the western side. Although suspicious, the measurements from Liepaja and Kolka will be kept for an initial model run. If bad model performance can be related to the low measurements the stations may be excluded.

Table 4 *Summary of wind speed characteristics at the LEGMC meteorological stations for the period 2004-2010.*

Station name	Max. speed	Average speed	Median speed	Available measurements
Liepaja	19.0	3.6	3.0	16 981
Pavilosta	13.0	2.8	3.0	16 470
Kolka	14.5	3.3	2.7	17 161

4.1.4 Finland

To assess whether winds in the Gulf of Finland are similar to those acting over the rest of the Baltic the wind direction measurements were subdivided into 8 directions. The results, seen in Chapter 4.1.5, showed that winds were once again predominantly SW or W.

The wind speeds were also compared in a similar way as for the previous stations, showing the Gulf of Finland to be slightly calmer than most of the other stations with an average wind speeds at 5.8 and 6.6 m/s and maximum speeds at 21.2 and 23.7 m/s.

Table 5 *Summary of wind speed characteristics at the FMI meteorological stations for the period 2004-2010.*

Station name	Max. speed	Average speed	Median speed	Available measurements
Russarö	23.7	6.6	6.1	19 886
Gråhara	21.2	5.8	5.6	20 169

4.1.5 Graphical presentation of wind directions

First the wind directions will be shown in Figure 12 as wind roses, intended to give the reader a visual impression of the directional distribution of the winds. Except for station Pavilosta in Latvia directions are similar not only between stations of the same country, but also over the entire Baltic region.

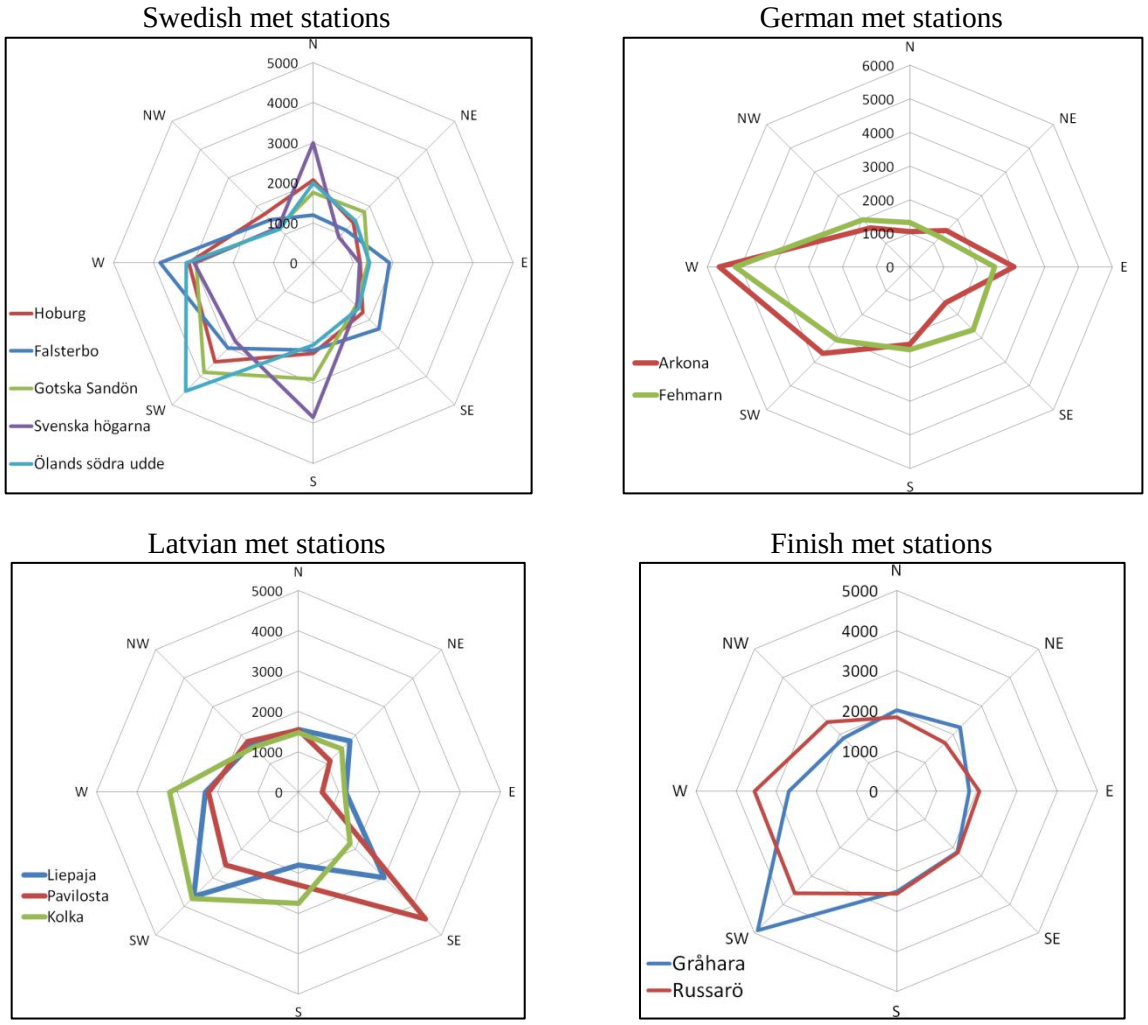

Figure 12 *Wind roses from the four countries supplying data for the study.*

Next the wind directions are presented in Figure 13 as cumulative bar charts, showing how large a percentage of the total winds each individual direction holds. It is once more striking how similar the distribution of wind directions is between the stations, with the exception of Pavilosta. The figure shows that for all trustworthy stations about 50% of the winds blow from the W/SW/S, making this the prevailing direction of the entire area.

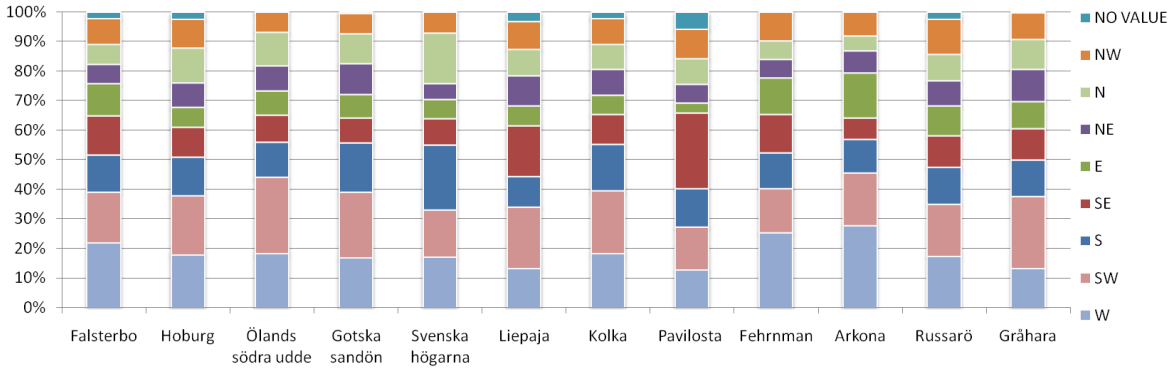

Figure 13 *Directions of winds at all the met stations used around the Baltic.*

4.2 Analysis of wave measurements

As mentioned five wave buoys had measurement coverage during 2004-2009, namely Arkona, Darss Sill, Södra Östersjön, Huvudskär ost and Finngrundet. Finngrundet is located in the Sea of Bothnia and is therefore not of interest. For the remaining 4 buoys a month in which all had measurements was found and is presented in Figure 14. The wave buoy Arkona is noteworthy as it presents much lower waves than nearby Darss Sill, only 80km away. In fact the highest value ever recorded at Arkona during 2004-2009 was only 2 meters, compared to the highest recorded wave at Darss Sill being 4.8 meters. It is not clear why wave buoy Arkona gave such low values as it does not appear to be sheltered and has fetches of 130 km to the SW and 50 km to the W, the two main wind directions of the area. Whatever the reason for the low values the buoy measurements are suspicious and will not be used for validation, leaving Darss Sill, Södra Östersjön and Huvdskär Ost as the only 3 buoys available for validation.

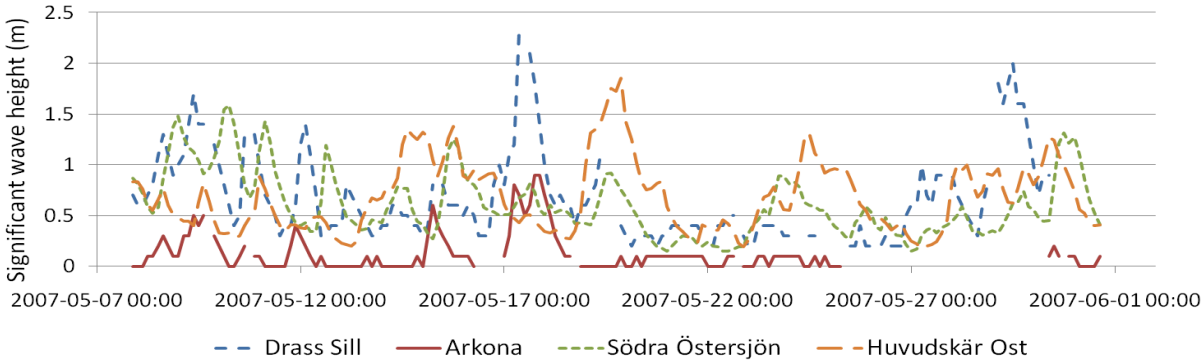

Figure 14 *Significant wave height measurements from the four buoys with measurement coverage for 2004-2009. Note how Arkona has much lower values than Darss Sill, even though they are only about 80km apart.*

4.3 Summary

- Winds blow from S/SW/W approximately 50% of the time.
- The meteorological station at Pavilosta, Latvia, was excluded from the study due to suspected local topographical effects on direction measurements.
- Latvian speed measurements seem suspiciously low compared to Swedish and German measurements.
- Average wind speeds in the area are between 5.8 and 7.5 m/s while maximum speeds are normally between 20 and 30 m/s (Latvian stations excluded on both parameters).
- Three trustworthy wave buoys have data coverage for the period 2004-2009. These are Darss Sill, Södra Östersjön and Huvudskär ost.

5 Adjustments of data and preparation for model run

5.1 Adjustment of bathymetric grid

WAM uses the grid properties of the bathymetric file as a base grid for its calculations. In order not to distort the calculations the version of WAM used in this study required quadratic grid cells, so the original 2x1 minute bathymetric grid had to be changed. When choosing the properties of the new bathymetric grid both the demand for regularity and the balance between accuracy and required computational time were taken into account. A higher resolution meant an increased accuracy and (hopefully) better results, but more grid points also meant longer computational times for each run.

The grid size found appropriate was 12x12 minutes, or 0.2x0.2 decimal degrees. At the southern end of the Baltic Sea this corresponded to a longitude step of ~13 km while it at the northern end corresponded to ~9.4 km. The latitude step remained ~22.3 km at both ends. The convergence of longitudes is due to the spherical shape of the earth, leading to a decrease in the metric distance between longitudes as one moves closer to the poles, while latitude steps remain constant. The new grid allowed for reasonable computational run times, while still maintaining a reasonable degree of detail, and the resulting grid points can be seen in Figure 15 a). The reduction of the grid was done by extracting every 6th longitude value (6*2'=12') and every 12th latitude value into a new grid. The new grid was then visually inspected to make sure no distortion had occurred.

As the scope of this study was limited to the southern Baltic Sea, it was desirable to leave the Sea of Bothnia out of the grid to further reduce the computational time. The validity of this exclusion will be discussed in detail in Chapter 6.2. The final bathymetric file was limited to only include grid points south of latitude 60.31^{o} as shown in Figure 15 b).

a) b)

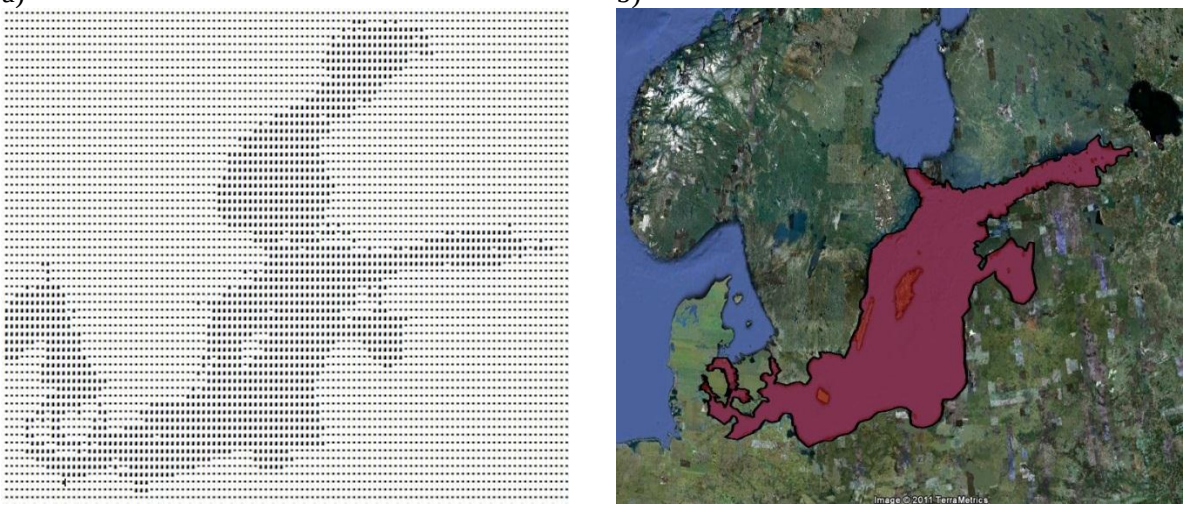

Figure 15 *a) The full resulting 12'x12' bathymetric grid used when running the model and b) the resulting area used when the Sea of Bothnia was excluded.*

5.2 Adjustments of wind data for WAM runs

The version of WAM used for this study could only read wind fields as U and V components in a standard Cartesian coordinate system with the *x*-axis towards east, the *y*-axis towards north and growing counter clock-wise. Winds are typically given according to standard meteorological convention in polar coordinates (wind direction and speed), with 0° as true north and growing clock-wise, and therefore had to be transformed to a Cartesian coordinate system. The two coordinate systems can be seen in Figure 16.

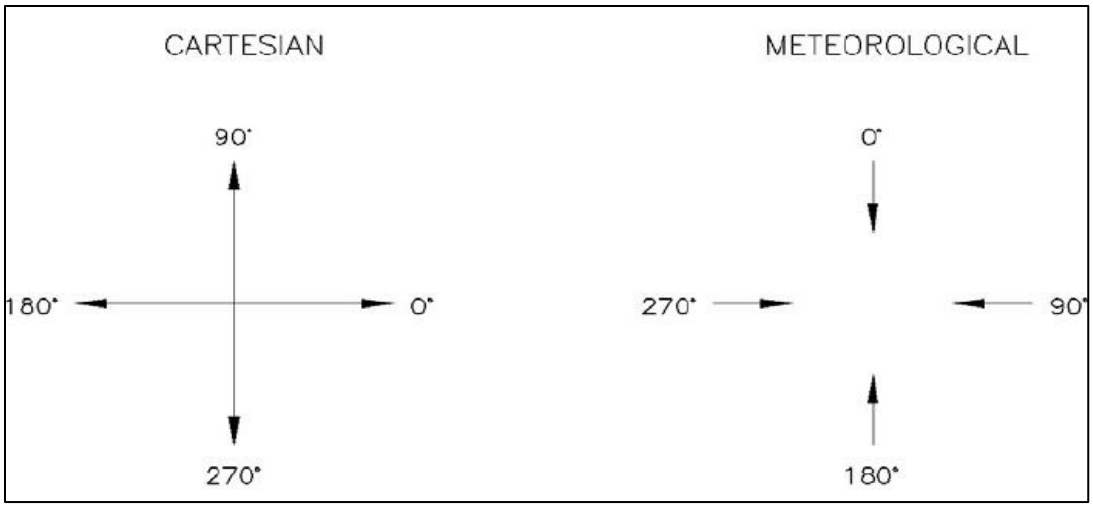

Figure 16 *Definitions of Cartesian and meteorological coordinate systems(CEM, 2006). Note that meteorological coordinates show which direction the wind is coming from, while Cartesian show the direction they are going to.*

The transformation between coordinate systems was done according to

$$U = -\cos\left((90° - \theta_{met}) * \mathrm{C}\right) * wind\ speed$$
$$V = -\sin\left((90° - \theta_{met}) * \mathrm{C}\right) * wind\ speed$$

$\theta_{met}$is the wind directions from the meteorological coordinate system and C is a conversion factor from degrees to radians, C=π/180.

For modeling purposes the wind speed used should always be that of a 10 m elevation equivalent wind, so whenever necessary a recalculation was done according to the equation below, taken from (SPM, 1984).

$$U_{10} = U(z)\left(\frac{10}{z}\right)^{1/7}, \mathrm{z} = \text{height of anemometer}$$

Winds measured in coastal regions are likely to be lower than winds blowing over open water due to the increased friction against land. Available literature suggests that overland wind speed measurements can be converted to equivalent open water velocities using Figure 17 a), derived from empirical results from the American Great Lakes (CEM, 2006). The figure shows the overland wind speed on its *x*-axis and the ratio between open water and overland velocities is on its *y*-axis. The figure shows how low overland wind speed measurement will be increased while wind speeds exceeding 18.5 m/s should be reduced by factor R_L=0.9.

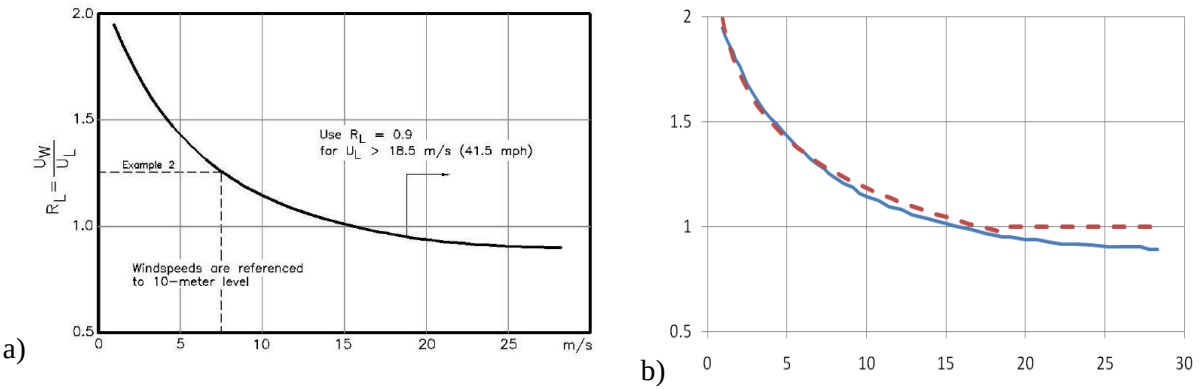

Figure 17 *a) Ratio between measured overland wind speed and equivalent open water velocity b) Digitalized version of the empirical curve from a) along with a logarithmically fitted curve (dashed). Values greater than 18.5 m/s are kept as they are.*

Figure 17 b) shows a digitalized result of the empirical curve presented in a). A logarithmic expression was fitted to the curve (dashed), allowing the empirical results in figure a) to be expressed as an equation. Although figure a) stated that wind speeds exceeding 18.5 m/s should be reduced, test runs showed that reduction of the high winds led to underestimation of the high waves. The reduction was therefore omitted and the final logarithmic formula for describing the conversion from overland wind speeds to open water wind speed was

$$\frac{U_W}{U_L} = \begin{matrix} -0.34\ln(U_L) + 1.9655 \text{ for } U_L < 18.5\ m/s \\ 1.0 \text{ for } U_L > 18.5\ m/s \end{matrix}$$

The possibility of altering the overland measurements will be used and further discussed in Chapter 7, when a validation of model results will be performed.

Another possible factor when converting land measurements to open water measurements is related to temperature differences between water and air. If nothing is known about the temperature difference it is customary to increase the wind speed by 10% (CEM, 2006). This factor was left out of this study as its effect falls between that of the different setups used, as will be seen in Chapter 7.2.

5.3 Allocations of areas of influence to wind measurements

The wind measurements supplied were only point-source measurements, and in order to use them for forcing WAM they were allocated areas of influence. The sum of the individual areas of influence covered the entire area modeled.

When allocating areas of influence to the stations the midway points between adjacent stations were found and marked (Figure 18) and the dots surrounding each station were connected to form a preliminary area (Figure 19). This created a number polygons between which non-allocated triangular areas arose, so the center-point of each such triangle was located and the surrounding areas were extended to meet in the center-point (Figure 20 and Figure 21). Once the boundaries had been found minor manual adjustments were made to assure that area limits fell on model grid points. A full map of the allocated areas can be seen in Appendix 2.

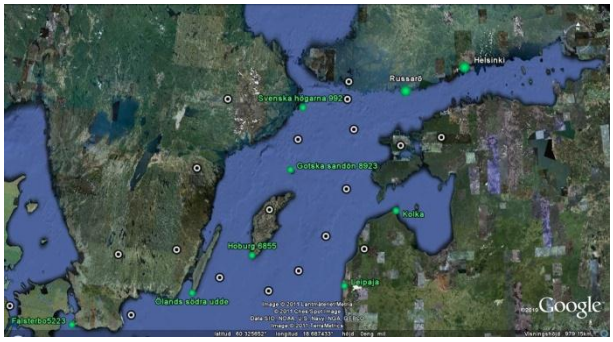

Figure 18 *Find and mark the half-way point between all measuring stations.*

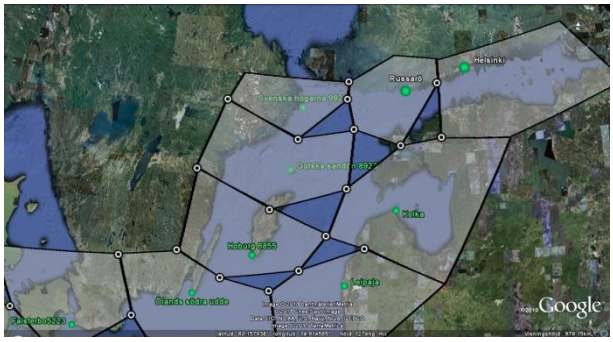

Figure 19 *Connect the half-way points of each station, forming an area of influence.*

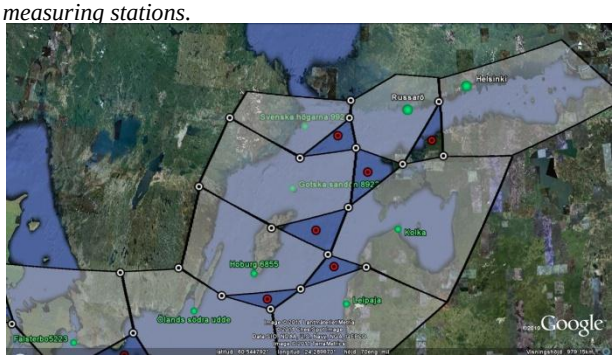

Figure 20 *Mark the center-point of the triangles that form between the areas of influence*

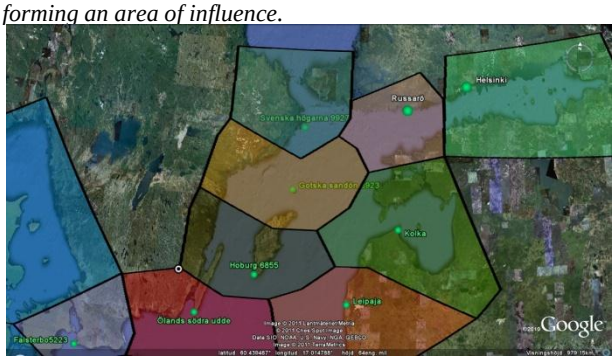

Figure 21 *Let the areas join together in the center-points, forming the final areas of influence.*

5.4 Preparation of wave buoy measurements

5.4.1 Sweden

The wave information supplied by the SMHI was given on an hourly basis, but as a model output time steps of three hours was desired the SMHI data had to be manipulated to be compatible to the model output. This was done by averaging the significant wave height over every three hour period by $\bar{x} = \frac{x_1+x_2+x_3}{3}$. Peak periods were averaged in the same way, while the direction of wave propagation was determined by selecting every third value. The different approach of the directional value was done to avoid the averaging problems involved in directions passing from 360^o to 0^o. If either of the three hourly values were missing the entire 3-hour period was assumed missing.

5.4.2 Germany

The German wave information was supplied in compact form, meaning that all missing values had been taken out of the data series. Although compact, this made comparison to other data set difficult, as it meant that two consecutive values in the German series did not necessarily correspond to two consecutive values in other sets. Dates were therefore added manually wherever missing, but with all parameter values stated as missing.

5.4.3 Latvia

No waves were used from Latvia

5.4.4 Finland

The wave information supplied by the FMI was not used due to their short period of coverage.

5.5 Summary

- The bathymetric grid was changed into a 12x12 minute grid, a resolution that will be used when the model is run. In the southern Baltic this corresponds to grid cells of ~13x22 km
- Winds were recalculated from polar values in a meteorological coordinate system into U and V components in a Cartesian coordinate system.
- Wind measurements were recalculated into 10 m elevation equivalent speeds when necessary.
- No correction for temperature instabilities between air and water was done.
- An equation for relating overland wind speeds to open water velocities was derived.
- Areas of influence were assigned to each meteorological station by joining midpoints of adjacent stations into closed polygons.
- Waves were recalculated into 3-hour averages to match the model output time step.

6 Sensitivity analysis

A sensitivity analysis was carried out to assess how quickly the model responded to a change in input parameters. The analysis focused on the calculation time step and on wind speed. It also assessed whether or not the omission of the Sea of Bothnia would affect the results in the southern parts.

6.1 Varying calculation time steps

Calculation time steps of 60, 120 and 180 sec were assessed with a test wind of 10 m/s rotating west-south-east over a period of 24 hours. 15 locations spread over the entire Baltic where chosen for comparison. Running this setup for the three different time steps rendered almost identical model results, with a maximum difference in wave height of only 2 cm. A table of the difference between the 60 sec time step and the 180 sec time step can be seen in Appendix 3. Since shorter time steps means longer runs without any major improvement of results the time step of 180 sec was chosen.

6.2 Omission of the Sea of Bothnia

As the Baltic Sea is divided into two almost individual water bodies by the narrow Åland straight it was hypothesized that the exclusion of the Sea of Bothnia would not affect the wave climate in the southern Baltic Sea. To test this hypothesis the model was run once with the full bathymetric grid and once excluding the parts north of lat 60.31° (approx north of Stockholm). No alteration was done to the bathymetry in the southern parts, so the Åland straight was still left open. The wind used was a 10 m/s wind rotating from west-south-east over a period of 24 hours.

Model results were assessed and compared at the buoy positions, but no difference at all could be detected, not even in direct connection to the cut (see Appendix 4 for results). This is assumed to be because wave energy from the southern Baltic was still allowed to escape through the straight. One could argue that waves moving north-south instead of south-north will have some effect on the wave climate, and that these waves are lost in the exclusion, but as winds are predominantly south-western this eventual loss of energy will be minor and not affect resulting waves in the southern parts.

6.3 Varying wind speeds

Three imaginary constant winds blowing from the SW (225°) were fed into the model. The wind speeds were 5, 10 and 15 m/s respectively. The wind was allowed to blow until a constant wave height was reached, and the wave heights were then compared. The results can be seen in Table 6, where the wave height for each wind speed is shown. The table also shows the normalized ratio between increase in wave heights and increase in wind speed. The normalisation was done by dividing the wave growth ratio with respect to the 5 m/s wave height by the wind growth ratio with respect to the 5 m/s wind speed according to

$$R_N = \frac{H_*/H_5}{U_*/U_5}$$

Table 6 *Resulting wave heights when increasing the wind speed. The table also shows the normalized ratio between wave height growth and the wind speed growth, R_N.*

	Resulting wave heights, H			Normalized ratio R_N		
Wind speed, U	**5**	**10**	**15**	**5**	**10**	**15**
Darss Sill	0.39	1.01	1.92	1.000	1.295	1.641
Arkona	0.47	1.30	2.45	1.000	1.383	1.738
Södra Östersjön	0.52	1.60	3.27	1.000	1.538	2.096
Northern Baltic	0.56	1.86	4.01	1.000	1.661	2.387
Huvudskär	0.51	1.63	3.50	1.000	1.598	2.288
Ölands södra grund	0.40	0.96	1.91	1.000	1.200	1.592

As the normalized ratio increases with increasing wind speeds this indicates that resulting wave heights do not grow linearly, as linear would mean a constant R_N. Figure 22 shows that the wave heights vary exponentially according to $H = \alpha * U^{\beta}$, where $\alpha \approx 0.030 - 0.042$ and $\beta \approx 1.41 - 1.79$. The locations with the higher waves are the locations with the longer fetches.

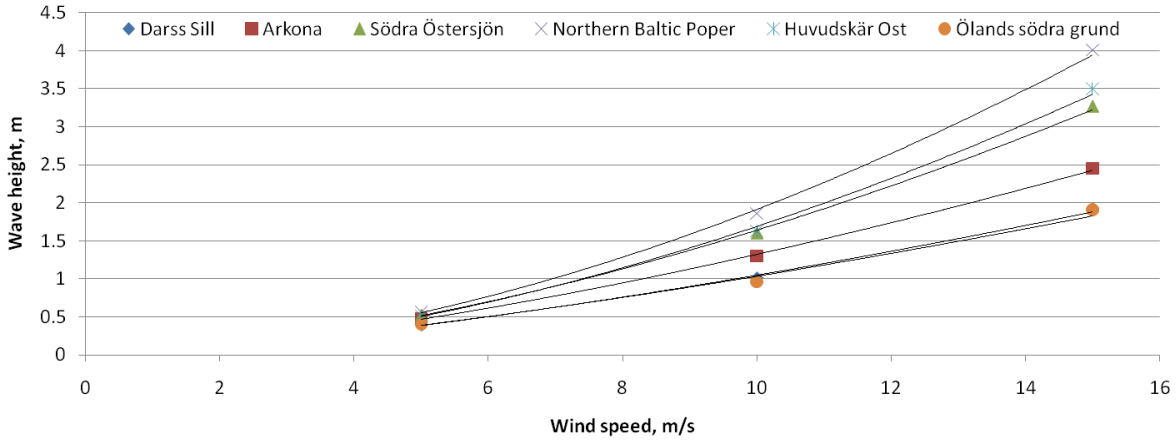

Figure 22 *Wind speeds plotted against resulting wave heights from the model.*

6.4 Summary

- Shortening calculation time steps has little influence on the final result. A calculation time step of 180 sec was chosen.
- Modelled wave heights increase exponentially with increasing wind speeds.
- Omitting the Sea of Bothnia from the bathymetric grid will not affect the results in the southern Baltic Sea and was therefore done.

7 Model validation

The validation of the model was done with respect to significant wave height, peak period and direction of wave propagation.

7.1 Statistics used for validation

Either time lines and/or scatterplots with linear regressions were used to validate the model's performance, depending on what was more illustrative. Each dot in a scatter plot represented a corresponding pair of buoy/model values, with the buoy measurement on the *x*-axis and the corresponding modeled result on the *y*-axis. If the modeled results had coincided perfectly with the measured results the scatter dots would have formed a straight 1:1 center-line of type $y = x$, but in reality scatter dots often form more of a cloud than a line. Through linear regression a straight line of type $y = kx + m$ was fitted to the scatter cloud based on a least mean square error technique, see *e.g.* (Moore, 1997) or (Vännman, 2002) for details, giving the modeler a tool to determine and compare the trends of different scatter clouds. The *k* value of the linear equation is called the regression coefficient, and deviations from *k*=1.0 showed the model's tendency to over- or underestimate results. An example of a scatter plot with regression lines can be seen in Figure 23

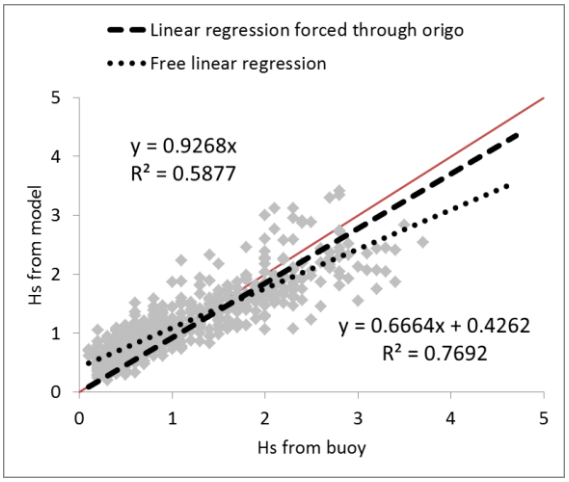

Figure 23 *Example of the two types of linear regression used. The dashed line is forced through origo, the dotted line is free us assume any m-value and the solid red line is the 1:1 center line.*

Linear regression alone was not enough to evaluate model performance as it does not state how representative the regression line was of the data within the scatter cloud. Through the coefficient of determination, also known as the R^2 value, it was possible to quantify the part of a variation recorded on a *y*-axis that derived from the linear regression equation and the corresponding variation on the *x*-axis. Put a little differently one can say that the R^2 value indicated how well the straight line embraced the data within the scatter cloud. R^2=1.0 means that all of the variation in the scatter cloud is described by the linear regression equation, *i.e.* the cloud is actually a line, while R^2=0 means none of the variation can be described by the regression line.

For this study two types of linear regressions were used, one where the linear regression was forced through origo and one where the *m*-value of the linear equation was free to assume any value. The forced regression made it possible to compare the scatterplots against each other while the free regression showed if there were any internal tendencies in the modeled results. Figure 23 gave an example of such a scatter plot. While the dashed line showed that the overall accordance between buoy measurements and modeled wave heights appeared good, the dotted line showed the internal tendency of overestimating small waves and underestimating larger waves.

7.2 Validation setups

Several validation runs were performed, starting with a 1 year run for 2007 to determine how well the model represented the general trends of the wave climate. This was followed by one "normal" run and two runs of extreme events to see in detail how WAM responded to

individual events. In an attempt to compensate for possible misrepresentations of the local wind measurements three different wind input setups were used for forcing the model.

Setup 1.

The 10 meter equivalent wind speeds, given as *U* and *V* components, were used. This setup showed how well the model represented reality when forced with "raw" point measurements from coastal areas.

Setup 2.

All wind speeds were increased by 20%. This derived from an often occurring underestimation of wave heights seen in several wave modeling studies. The value 20% has some basis in previous experiences (Bertotti, 2011), but should be considered as arbitrarily chosen for this study.

Setup 3.

All winds were recalculated using the logarithmic expression found in Chapter 4.1.5 for conversion of overland measurements to open water measurements. This expression was appealing both in its scientific and logical validity as low wind speeds were increased more than high ones. As the sensitivity analysis showed that resulting wave heights grew exponentially with increasing wind speed the weighted increase of the logarithmic expression was expected to bring up the wind speed under normal circumstances without overestimating wave heights during storm events, a clear risk when using the unweighted Setup 2.

Before presenting the results of the validation runs discussed above the author wishes to remind the reader of the suspiciously low wind speed measurements previously noted for Latvian stations. If the speeds are indeed bad representations of the wind fields over the eastern Baltic Sea, their inclusion will distort model results.

7.3 Influence of Latvian weather stations

To best assess the influence of the low Latvian wind speeds a period in which winds blew from the east was chosen. The buoy chosen for the validation was that most affected by the Latvian winds, *i.e.* Södra Östersjön.

Figure 24 a) shows buoy measurements and model results of H_s along with wind speed measurements taken on both the Swedish and Latvian coasts. Note how the Latvian wind speeds were considerably lower. In Figure 24 b) the wind speeds were substituted for wind directions, note how the wind shifted from westerly to easterly. Combing a) and b) showed that although the wind speeds were constantly lower on the Latvian side it was only while winds were easterly that there was any difference in the model results. Even then the differences were surprisingly small, only about 10-15%.

As Chapter 4.1 showed winds to be mainly from SW it would make little difference for the results on the Swedish coast if the Latvian stations were included in medium-term modelling or not, but as the results were a little bit better when the Latvian stations were excluded they were taken out of all further modelling. Their areas of influence were taken over according to Appendix 2.

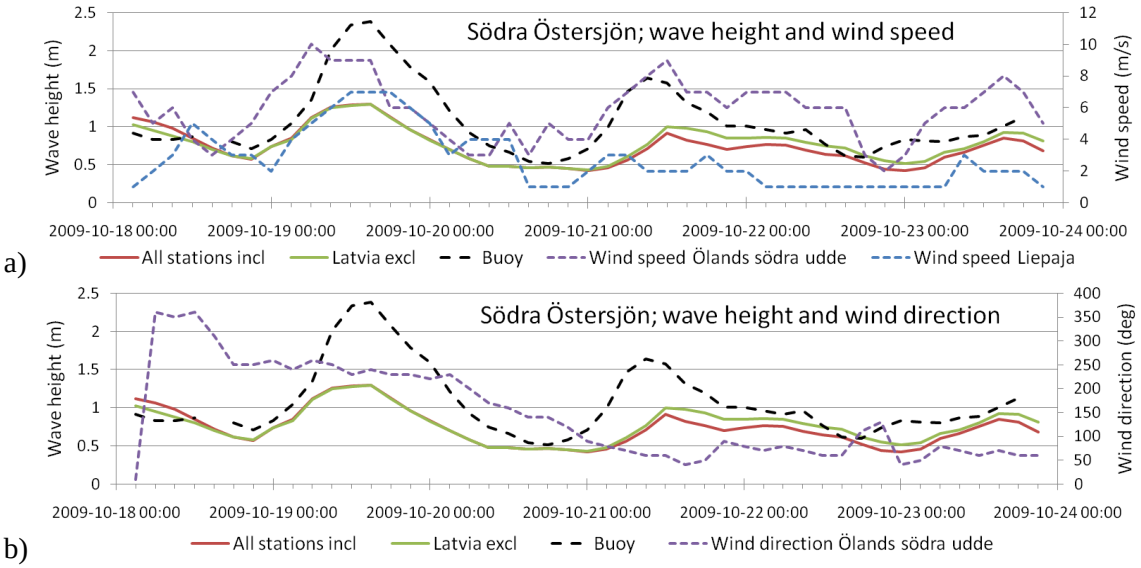

Figure 24 *a) measured and modeled wave heights, along with a wind speed measurement from either side of the Baltic. b) Same as a) but with wind speed substituted for wind direction. Note how model results start drifting apart as the wind turns from westerly to easterly*

7.4 One-year validation for 2007

By validation of a whole year a fair idea of the model's general behavior was gained. Resulting scatterplots, seen in Figure 25, showed that when forced with the unchanged winds WAM generally underestimated the resulting wave heights. Both the logarithmic expression and the 20% increase in wind speed rendered better regressions, falling closer to the 1:1 line. The non-linear nature of Setup 3 was clearly seen in the internal tendencies of the clouds, where low waves grew more than high waves. The resulting regression coefficients and R^2 values have been summarized in Appendix 6. Note especially how the regression coefficients are similar between Setup 2 and 3 but the R^2 values are considerably better for Setup 2 due to the previously mentioned tendencies of Setup 3. When comparing the R^2 values between the buoys it can be seen that Darss Sill, a buoy representing a relatively small area with several wind measurements, has better values than Södra Östersjön and Huvudskär ost, both representing much larger areas and with fewer measurements. The weakness of a larger area was particularly visible for Södra Östersjön where the green circles in Figure 25 mark buoy measurements for what must have been very rough winds (H_S 4 to 5 m) but with only moderate model results (H_S 2 m). In this instance the land measurements used to force the model were obviously not representative of the full area, even if strong winds must have been blowing.

The lacking internal distortion of Setup 2 made this Setup seem like an appealing option, but a closer look at the scatterplots revealed that while the general fit was good Setup 2 suffered from substantial overestimations (nearly 100%) of certain high waves, marked as red circles in Figure 25. This was probably a result of local wind measurements occasionally being stronger than the winds acting over the whole area of influence, a difference increased a further 20% by the setup. Due to the previously mentioned exponential growth in wave height with respect to wind speed the results of these exaggerated winds were seen as the further exaggerated waves. This meant that Setup 2 gave the best general description of the waves, but with great uncertainty concerning the highest waves, something well worth remembering when the final Setup is chosen.

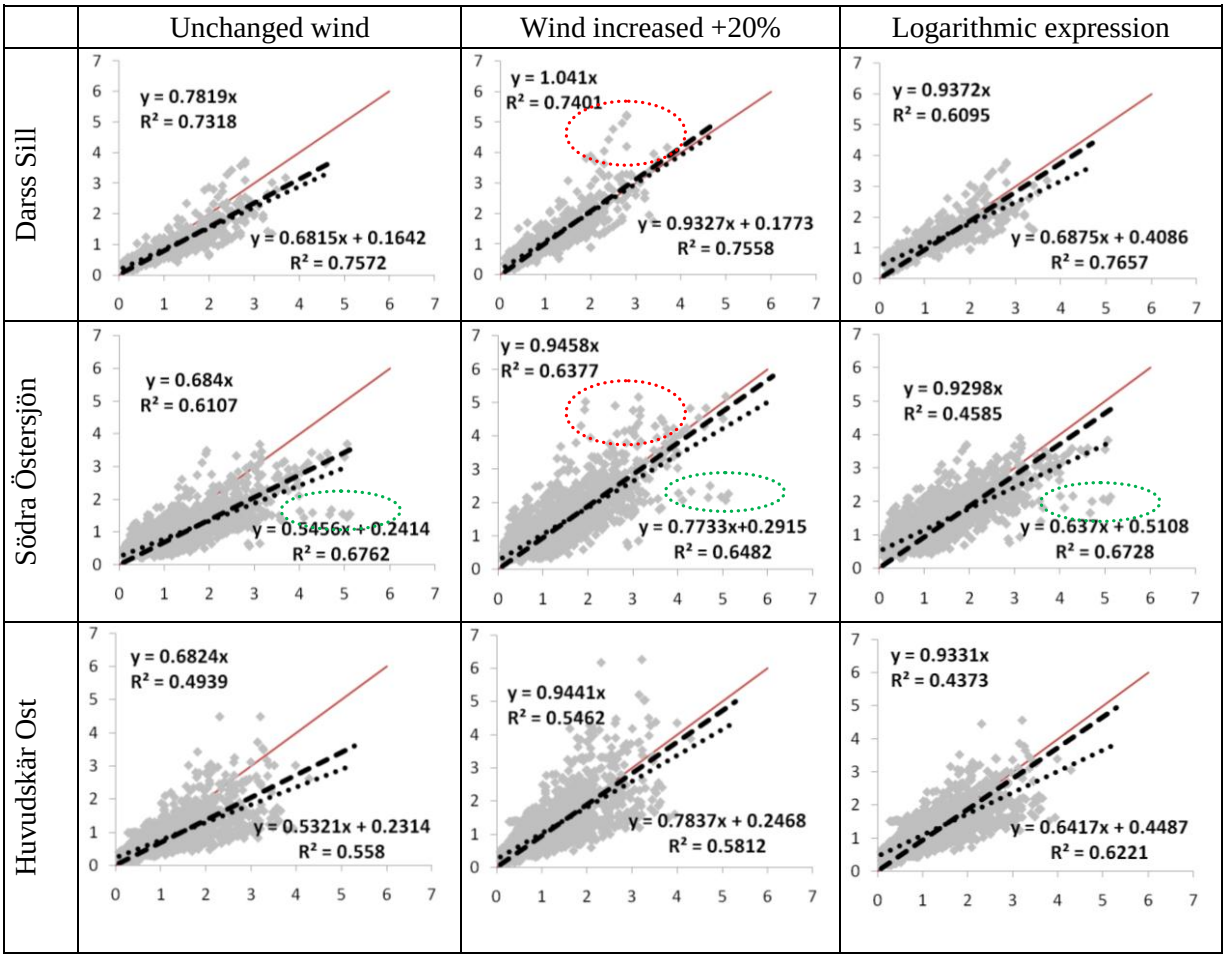

Figure 25 *Scatterplots of H_S for the three validation points during 2007. Buoy measurements are on the x-axis while model results are on the y-axis. The red solid line is the 1:1 center-line, the dashed line is a linear regression forced through origo and the dotted line is a free linear regression. Red circles mark events of highly exaggerated model results, while green circles show events where the model missed high waves due to locally lower wind measurements.*

For the direction of wave propagation a graph of the full time series can be found in Appendix 5. In Figure 26 the scatterplots of the wave direction for Södra Östersjön and Huvudskär ost are presented. The regression lines have been excluded from the graphs as the equality of values 0^o and 360^o makes regression misleading. Darss Sill was not included as no directional measurements were obtained there. The plots show that the model generally did a good job of describing the direction of wave propagation. A visual comparison showed that the scatter increased somewhat for Setup 3 and that Södra Östersjön shows less agreement than Huvudskär ost.

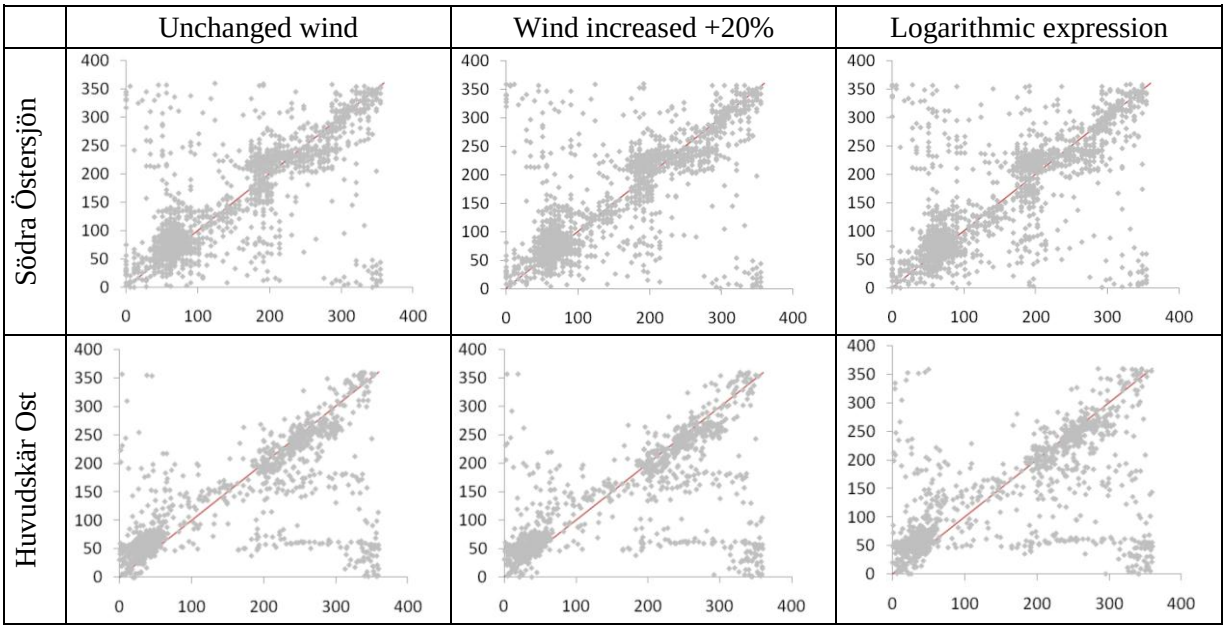

Figure 26 *Scatterplots for direction of wave propagation. Buoy measurements are on the x-axis while model results are on the y-axis.*

For the peak periods a scatter plot comparison can be seen in Figure 27. It was difficult to determine the applicability of the model results just by looking at the scatterplots as the analysis showed a good result for the regression line, but with substantial spreading of the scatter dots. By comparing the scatterplots to a time line of the results, found in Appendix 5, it was possible to determine that the overall fit of the model results were acceptable, but with individual results at times being quite bad. Luckily, in most applications the sensitivity to the peak period is considerably lower than to the other two parameters.

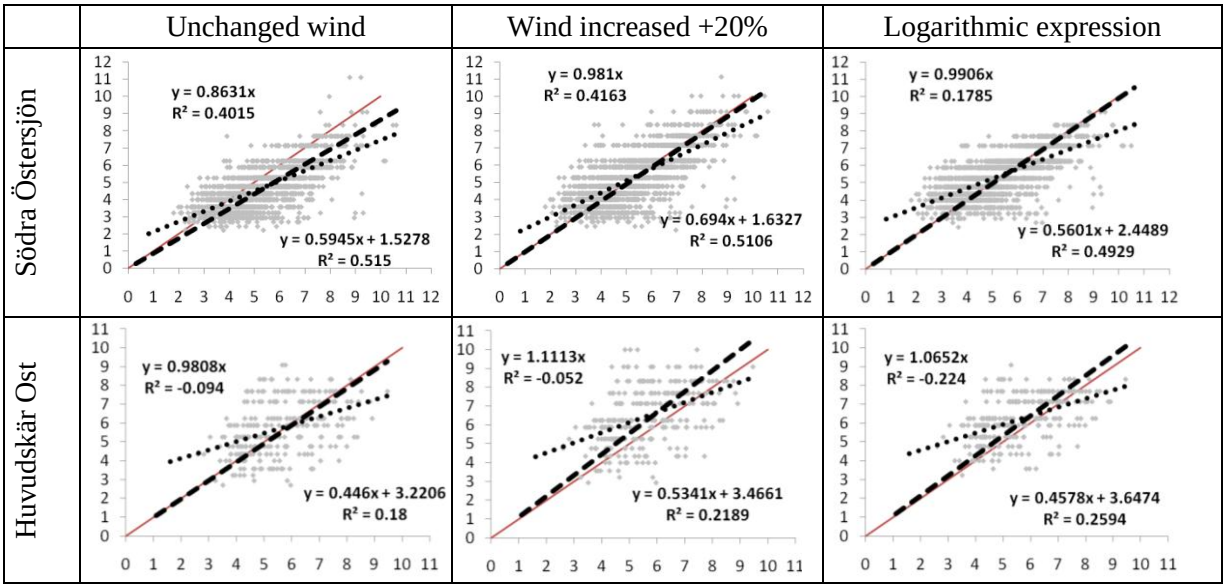

Figure 27 *Wave peak period.*

7.5 Validation October 2009

To look at the model's performance under "normal" circumstances a week in October 2009 was chosen. Wind speeds were between 4 and10 m/s during most of the period for all three areas. A first impression of model performance for H_s can be obtained from Figure 28, showing how modeled results generally follow the same trends as the measured ones, but with incorrect magnitudes. Södra Östersjön showed the biggest difficulties, at times underestimating the wave height by more than a meter. The waves' strong dependence on the wind can clearly be seen at Darss Sill on Oct 21st.

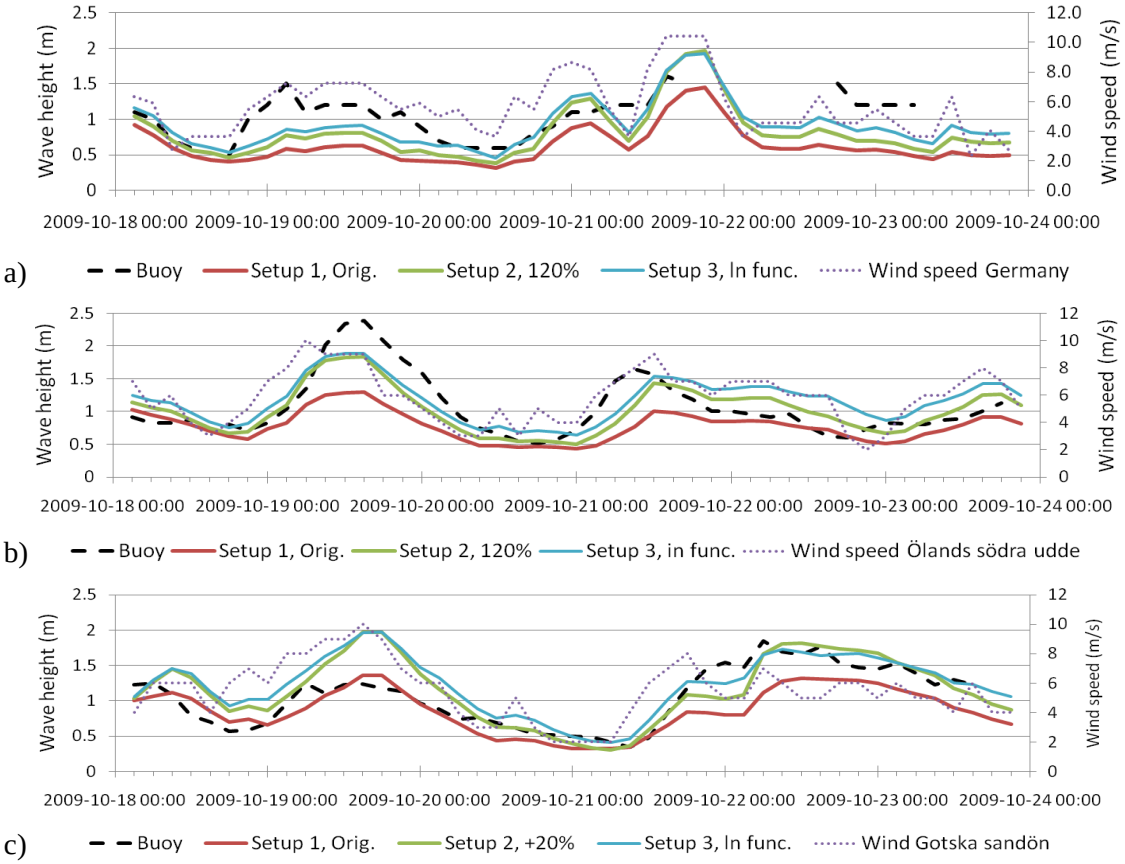

Figure 28 *Graphic illustration of H_s at a) Darss Sill b) Södra Östersjön and c) Huvudskär ost. Along with H_s the graphs also show the wind speeds generating the waves. Note the waves' fast response to change in wind speed.*

In Figure 29 the values from the graphs are presented as scatterplots. For Setup 1 the results of the forced regression lines were unsatisfactory at both Darss Sill and Södra Östersjön with regression coefficients of 0.58 and 0.67 and R^2 values of 0.38 and 0.21. The very low R^2 value of Södra Östersjön is also reflected in the large difference in slope between the free and forced linear regressions, indicating large internal variance from the forced regression line. A table of the regression coefficients and the R^2 values can be found in Appendix 6.

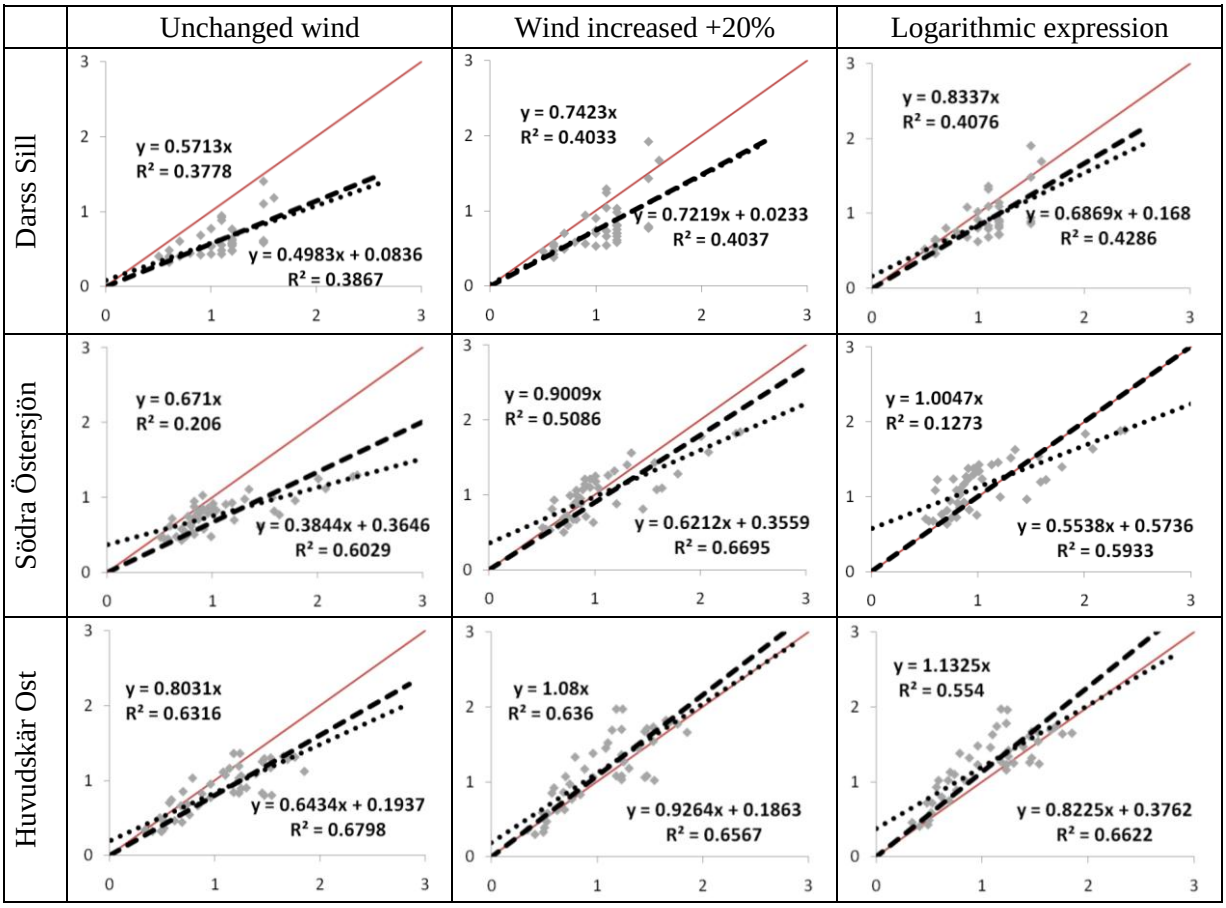

Figure 29 *Scatterplots for H_s for the three different setups at the studied locations. Note especially the low accordance for Setup 1, and the similar regression coefficients between Setup 2 and 3 but better R^2 values for Setup 2.*

Setup 2 and 3 gave better regressions for both Darss Sill and Södra Östersjön, but still with low R^2 values, and still failing to reach the measured peak on the 19th. This suggests that the wind measurements used to force the model were simply not good enough representations of the wind blowing over the open water. For Huvudskär Ost Figure 28 showed that Setup 1 caught the low peak on the 19th very well, but underestimated the high peak around the 23rd, while Setup 2 and 3 acted in the opposite way. This again points to the land measurements not being complete representations of the open water wind conditions.

Graphs of the directions of wave propagation can be seen in Figure 30 a) and b). Although the timing of the model was a bit off the model had no problem in regenerating the general shape of the measurement curve. Some differences could be noticed between the three setups, but they were minor and inconsistent.

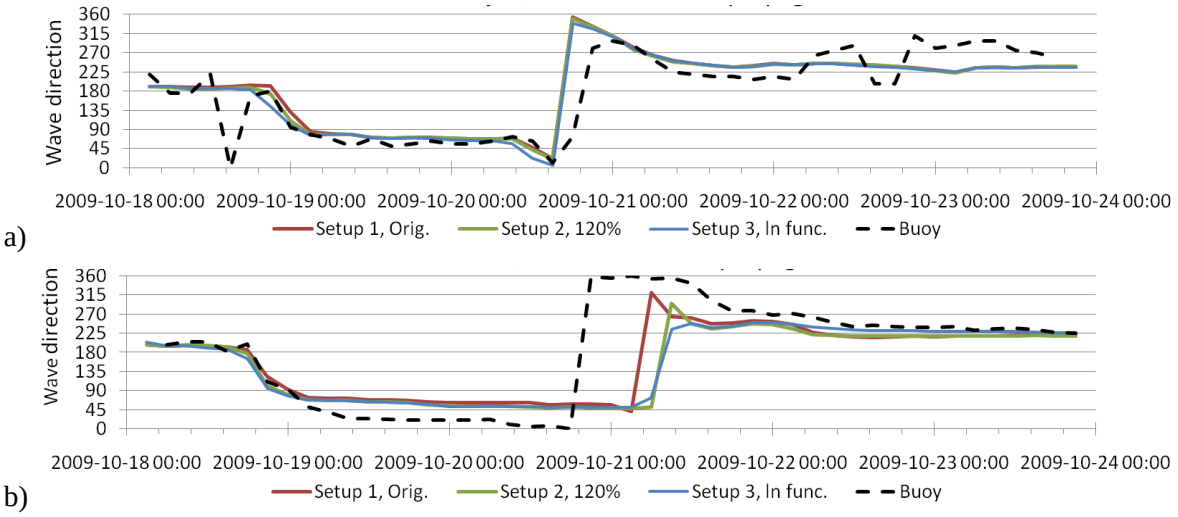

Figure 30 *Direction of propagation at a) Södra Östersjön and b) Huvudskär ost.*

For the peak periods measurements were only available at Södra Östersjön. A graphical illustration of the results can be seen in Figure 31 along with the scatterplot in Figure 32. By visual comparison it seemed as if Setup 3 had the best accordance to the measurements, even if it missed the timing of a peak around the 23rd. The scatterplots also showed that Setup 3 gave the best regression, but the large spreading of the dots gave the impression that model results were almost random. By looking at the timeline once more it was quickly determined that the model performance was not as bad as it seemed from the scatter plot, it was simply a bit off in its timing.

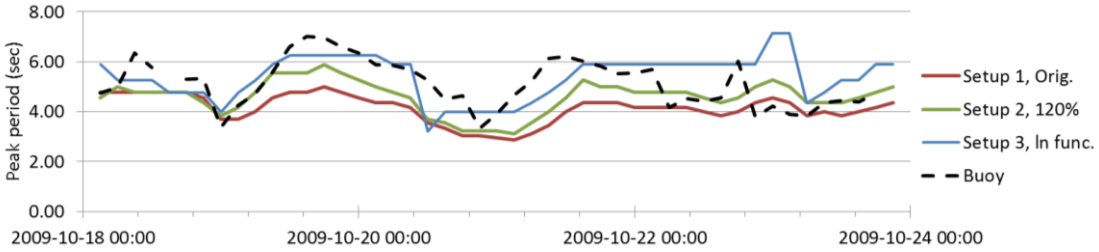

Figure 31 *Peak period at Södra Östersjön.*

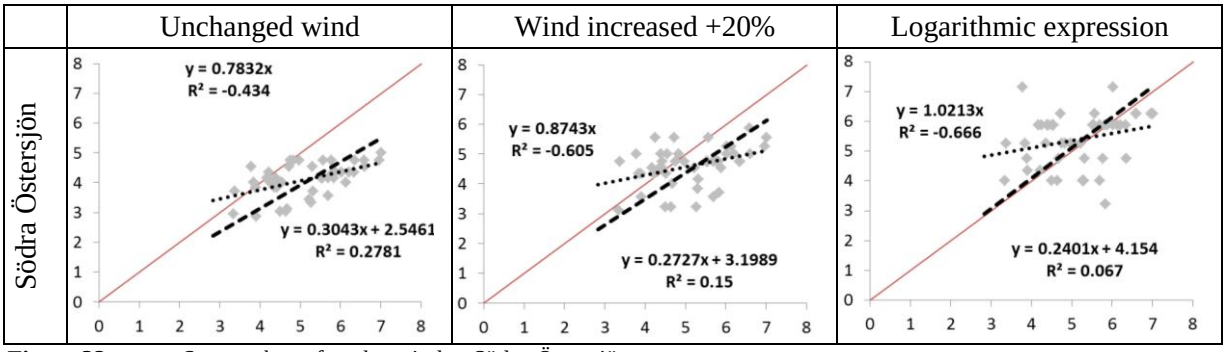

Figure 32 *Scatterplots of peak period at Södra Östersjön.*

The concluding remark from the October 2009 validation runs will be that the model has some difficulties in correctly regenerating the wave height during periods of weak winds. This is probably due to increased local differences in winds, leading to local measurements being less representative of large areas. Wave directions are still represented reasonably well, but with some inaccuracy in their timing.

7.6 Validation for storm Gudrun

In January of 2005 a severe storm passed over southern Sweden. The storm, named Gudrun, had gusts of up to 42 m/s and was the most destructive storm ever recorded in Sweden (SMHI, 2009c). A storm of this magnitude presented a good opportunity of evaluating how the model reacted to extreme events. Unfortunately buoy measurements were only available from buoy Darss Sill.

Figure 33 shows the modeled results of the three different setups, along with the measured buoy values (dashed line) and a wind speed measurement from the German coast (dotted line). The figure shows how the pattern of the measured wave growth/decline is represented well by all setups, but with varying accuracy in the magnitude. It also gives a good illustration of the model's reactions to Setup 2 and Setup 3 during storm event. At wind speeds around 5 m/s the difference in wave height between the two setups was hardly notable, but as the speed increased the difference grew to several meters. This clearly illustrates the reason for including the logarithmic expression as potential local overrepresentations of wind speeds are further enhanced and applied to the entire area by Setup 2. Such overrepresentations may be rare, but as the top-end of the wave heights is the final aim their impact could potentially be great. For case Gudrun however, Setup 2 provided a better overall result than Setup 3

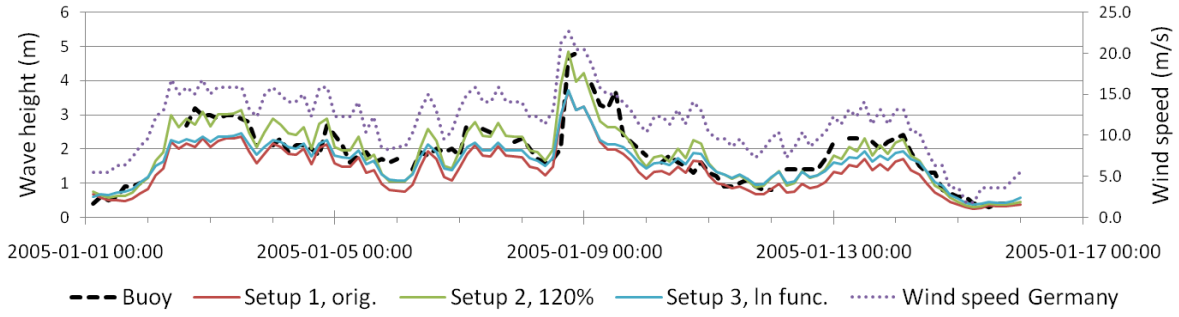

Figure 33 *Significant wave height at Darss Sill during the January storm of 2005.*

In order to numerically compare the setups their scatterplots are presented in Figure 34. Once again Setup 2 gave the best fit to measured values with a regression coefficient of 0.99 and an R^2 value of 0.81. The free regression showed next to no tendencies of internal distributions differing from that of the forced regression.

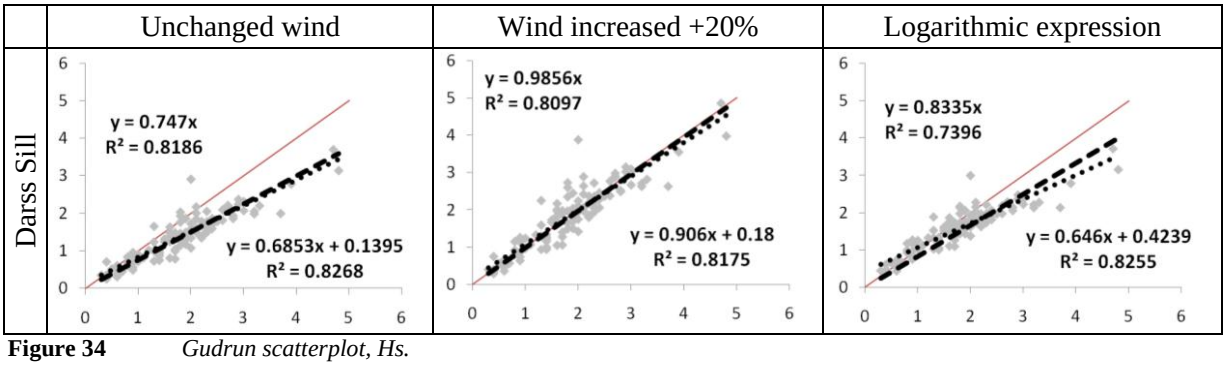

Figure 34 *Gudrun scatterplot, Hs.*

In conclusion it seems as if the model captured the storm event well, and it is particularly noteworthy how already the unchanged winds of Setup 1 gave a good representation with high R^2 values. This indicates that land measurements seem to be more suited for forcing the model under strong wind conditions, probably due to an increased homogeneity of the wind field during storms.

7.7 Validation for storm Pär

In Jan 2007 a second sever storm hit Sweden, this time named Pär, with gusts reaching just under 30 m/s. For storm Pär wave measurements were available at Darss Sill and Huvudskär ost. An overview of the model results can be seen in Figure 35, along with the wind speed measurements. Once again the patterns of wave growth were represented well, but with incorrect magnitudes. At Darss Sill Setup 2 captured the higher waves better than Setup 3, but at Huvudskär ost Setup 2 overestimated the wave height by almost 3m, much more than Setup 3.

a)

b)

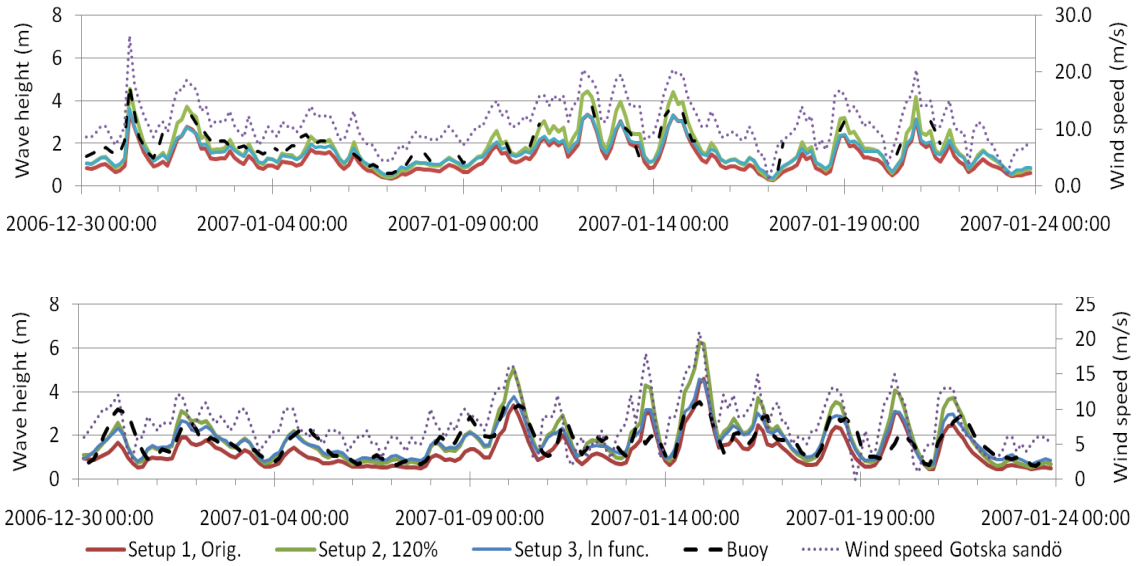

Figure 35 *Significant wave height at a) Darss Sill and b) Huvudskär ost during the January storm Pär of 2007.*

The scatterplots in Figure 36 show that for Darss Sill the storm event was described in a satisfactory way, especially for Setup 2 with a regression coefficient of 0.92, an R^2 value of 0.76 and very little internal distortion. For Huvudskär ost the results were less promising, with R^2 values of only 0.35-0.45 for all three setups. The low accordance was due to the several instances of exaggerated model wave peaks, seen already at Setup 1. The model peaks are believed to derive from local winds being stronger than the regional ones.

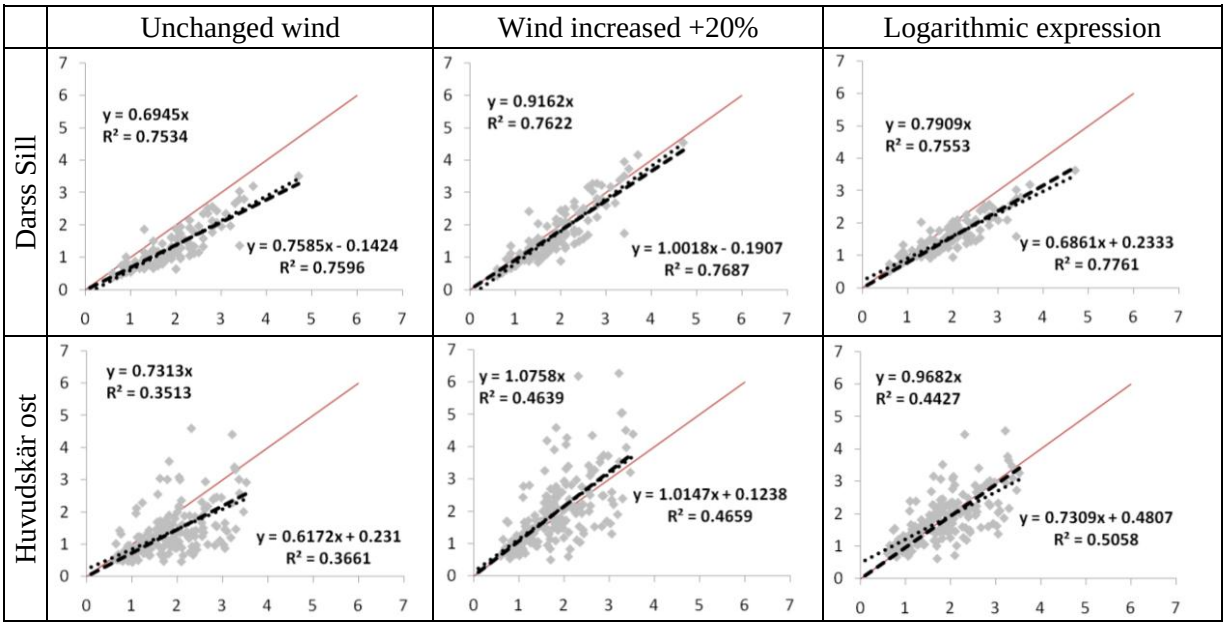

Figure 36 *Scatterplots of Hs during the January storm Pär of 2007.*

For the direction of wave propagation and the wave peak period only Huvudskär ost was available for validation, as these parameters were not measured at Darss Sill. The directions of propagation, seen in Figure 37, showed the same trend as for the weaker winds, with a good general accordance but slightly incorrect timing and with only minor differences between setups. Also the peak periods follow the same pattern as for the weaker winds, with a good general fit but incorrect values, something further shown by the scatter plot.

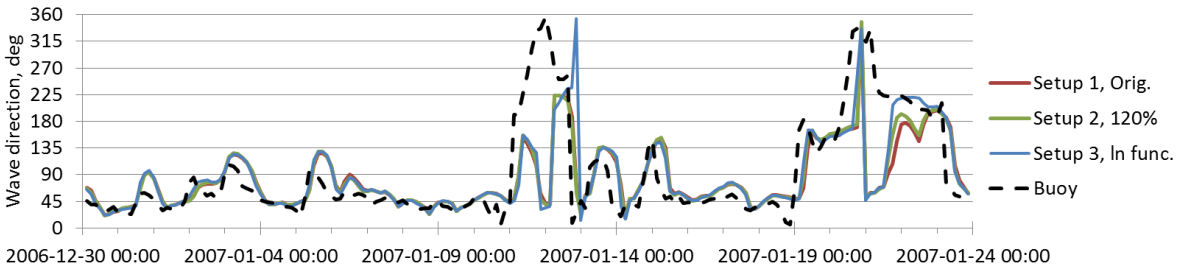

Figure 37 *Direction of propagation at Huvudskär ost during storm Pär.*

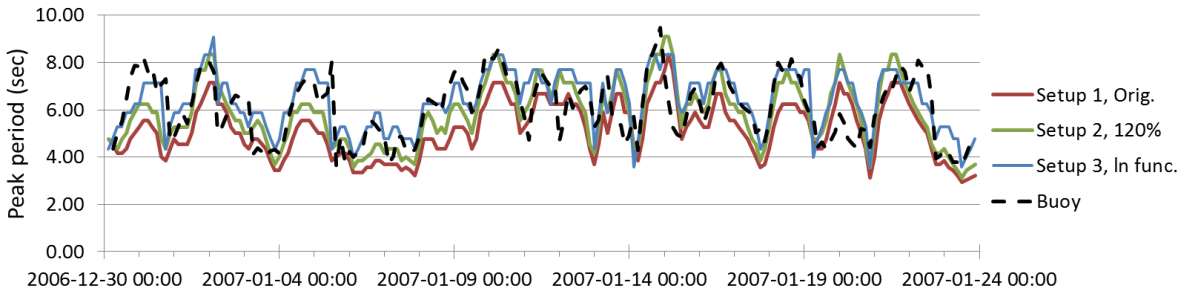

Figure 38 *Peak periods at Huvudskär ost during storm Pär.*

	Unchanged wind	Wind increased +20%	Logarithmic expression
Huvudskär ost	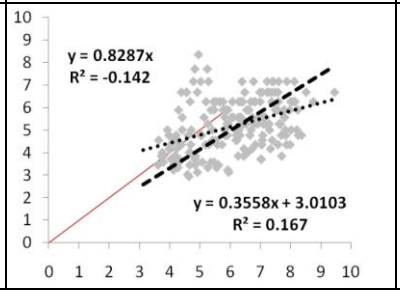	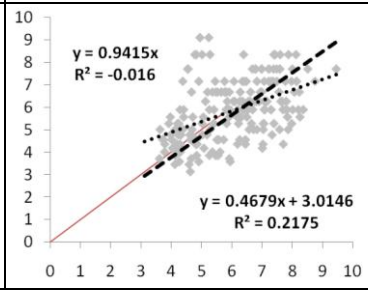	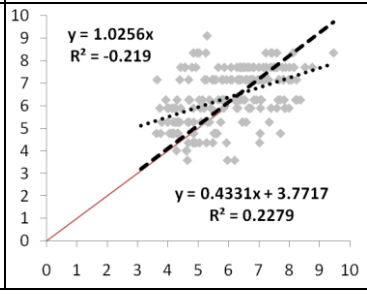

Figure 39 *Scatterplots for peak periods during storm Pär.*

In conclusion, the strong winds continue to give good model results at Darss Sill already at Setup 1. Even so, the low agreement seen at Huvudskär ost shows that strong winds are in themselves no guarantee that the winds on land and over open water will be equal.

7.8 Summary

- All the Latvian stations were excluded from the study
- Winds were prepared according to three separate Setup schemes before used for forcing the model.
- Periods of strong winds seemed to give better accordance for wave heights than periods of weak winds, most probably due to a low degree of local variations.
- The bigger the area over which a wind measurement was averaged, the larger the spread of the scatterplots. This meant that Darss Sill gave more trustworthy results than Södra Östersjön and Huvudskär ost.
- Setup 2 gave the best overall fit to buoy measurements, but risked heavily overestimating waves. Setup 3 gave a similar general fit as Setup 2, but without the strong overestimation
- Directions of wave propagation were regenerated in a satisfactory way for all setups.
- Peak periods showed substantial variation in accuracy within the data, but gave a good average representation. This was consistent for all three wind setups.

8 Setup chosen for further modelling

Based on the results of the validation runs it was concluded that local wind measurements can indeed be used to force the wave model and find wave climate statistics, if modified according to Setup 3. Setup 1 consistently gave too low results and was quickly abandoned, but the choice between Setup 2 and Setup 3 was not as easy. Setup 2 gave better results most of the time, but had a tendency to heavily overestimate the top portion of the wave heights. As this is the part of greatest interest for the wave statistics it was seen as too uncertain to include these waves. Setup 2 was therefore abandoned, leaving Setup 3 as the final choice. Neither the results from comparison of propagation directions nor peak periods were to the disadvantage of Setup 3.

It must be understood that wave statistics resulting from forcing the model with local winds modified according to Setup 3 will suffer several uncertainties. Due to local variability in wind fields a wind's ability to represent a larger area at any given time can not be guaranteed, and individual events can not be picked out of the long term analysis and expected to be accurate. It is, however, probable that a general idea of the individual event could be gained. Stronger winds tend to give a more accurate description of larger areas, so there are good prospects for correct representation of high waves.

9 Results

Chapter 9 starts off by discussing model results at the buoy locations to ensure that model performance has not deteriorated with the longer model run. Both scatterplots and monthly average values will be used to ensure the maintained reliability of the model. After this the results at the five selected locations discussed in Chapter 1.3 will be presented in an accessible form intended for easy practical use.

9.1 Model performance at buoy locations

No major differences can be seen in the resulting scatterplots between the 1-year run and the 6-year run. Both regression coefficients and R^2 values are very similar for H_S, and the internal tendencies still show a general overestimation of low waves and underestimation of the top-portion. The directional agreement remains good, while the peak periods remain difficult to interpret. These results suggest that model output is applicable for determining the medium-range wave climate of the southern Baltic Sea.

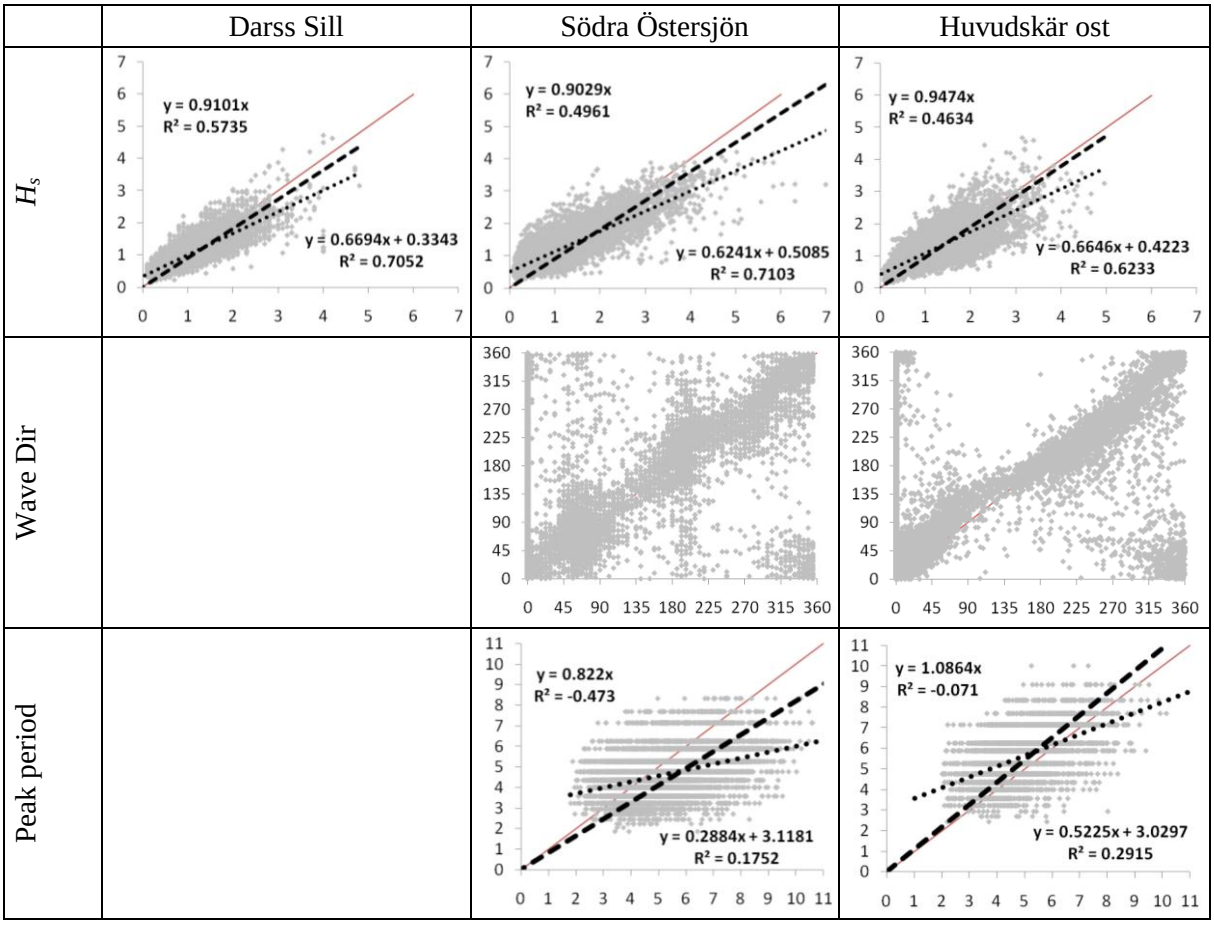

Figure 40 *Scatterplots of the 6 year run between 2004 and 2009.*

The agreement between the model results and the buoy measurements can also be shown by comparing their average monthly values. This is done in Figure 41. Each color in the figure represents a buoy location, where the left bar shows the model result at the location and the right bar shows the buoy measurement results. The good accordance between model and measurement shows the model performance to be both solid and good. The slight underestimated of H_S for high waves and slight overestimation for low waves can still be seen.

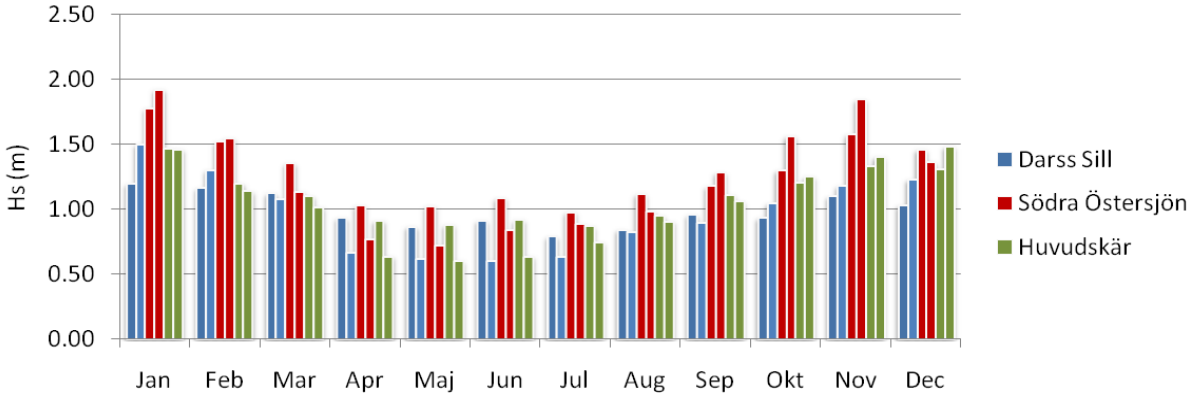

Figure 41 *Average monthly values of Hs. The left bar shows model values while the right bar shows values based on buoy measurements.*

9.2 Wave height at selected locations

The resulting significant wave heights at the five selected locations discussed in Chapter 1.3 are presented in Figure 42 to Figure 44. The significant wave height has been presented in three different ways, intended for three different types of applications. First the average values of H_S are presented on a monthly basis, illustrating typical conditions. After this, the average value of the top 10 % of H_S are presented, intended to illustrated rough but not extreme conditions. Finally, the maximum model results for H_S are presented, intended to be used as guidance on extreme events in design situations.

For the average values of $H_{S,}$ seen in Figure 42, it is striking how similar the wave height patterns are at all five locations, clearly suggesting that the winds used to force the model were indeed similar over the entire area. The figure also shows that April to August is generally a period of lower waves while November to February is a period of higher waves and that the sheltered areas of Hanöbukten and near Öland experience lower waves than the more exposed and open areas around Falsterbo, Ystad and Nynäshamn. The highest average waves were seen at Nynäshamn, just as the strongest winds were measured at Svenska högarna. Nynäshamn is also the location with the longest fetch. These results lend credibility to the model output.

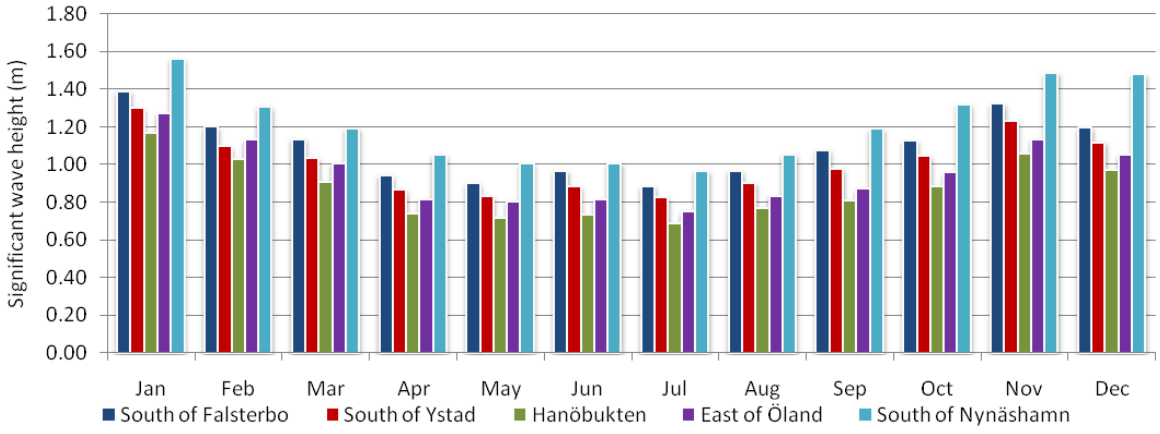

Figure 42 *Average values of the significant wave heights resulting from the model.*

For the rough weather conditions, illustrated in Figure 43, the annual cycle is similar to that of the average waves, but with a noteworthy exception. In June both Falsterbo and Ystad suffer from rough weather waves that are more than half a meter higher than those at Hanöbukten. These higher waves demonstrate how locally strong winds seem to be reoccurring in June at the southern tip of Sweden. The locally high waves become even clearer when looking at the

maximum wave heights, illustrated in Figure 44, were it can be seen that the maximum value for Falsterbo is 2 m higher than that of Hanöbukten in June.

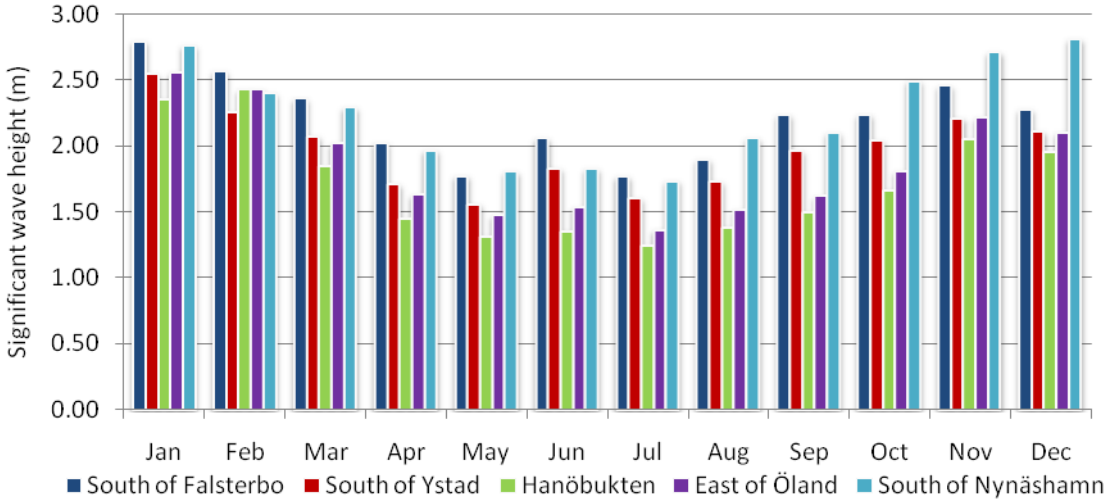

Figure 43 *Average values of the top 10% of significant wave heights resulting from the model.*

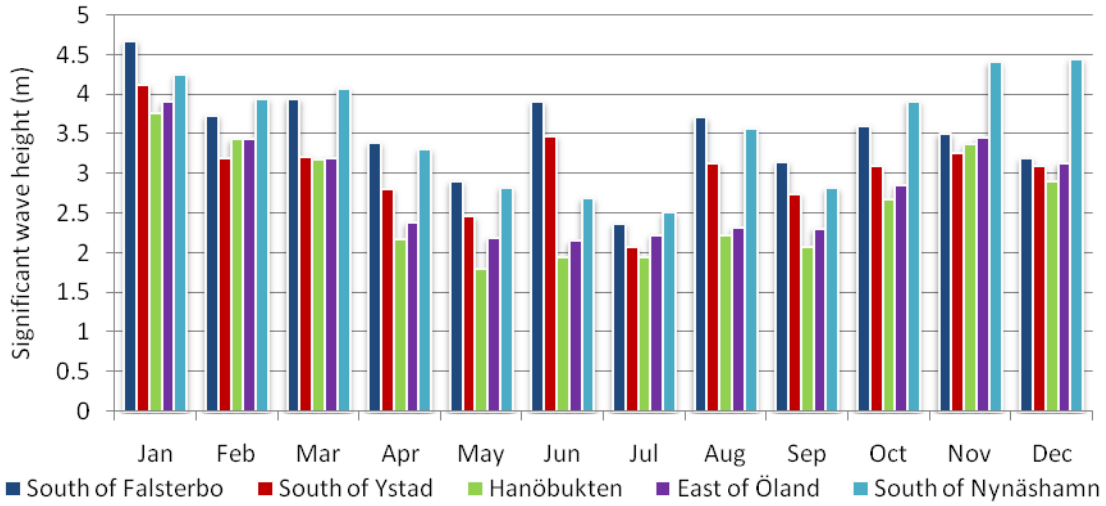

Figure 44 *Maximum significant wave heights resulting from the model.*

In a design situation it is rare to design a structure or a system to withstand very extreme events, as this would become unreasonably expensive. It is therefore desirable to determine how large a percentage of the incoming waves that will exceed any given H_S, and to this end the cumulative distributions of the wave heights at the five locations have been presented in Figure 45. The figure shows how the limiting H_S exceed by *e.g.* 20% of the waves at Hanöbukten is 1.25 m while at Nynäshamn it would be 1.75 m. Reversing the reading of the graph one can also conclude that a structure withstanding a 2 m wave would withstand 97% of the waves at Hanöbukten, but only 91% of the waves at Nynäshamn.

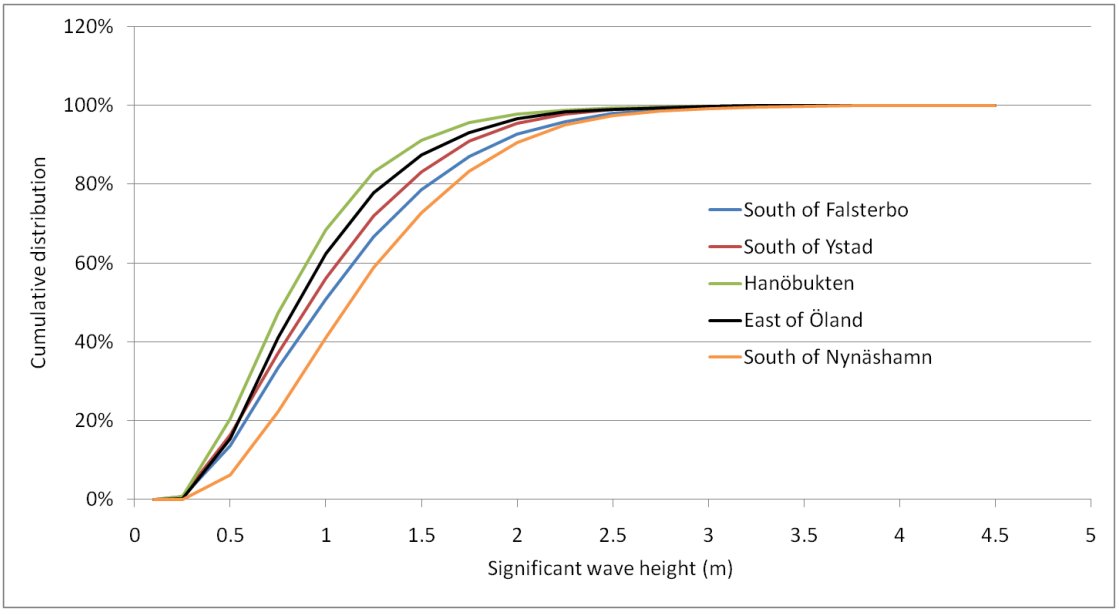

Figure 45 *Cumulative distribution of the wave heights at the five selected locations.*

Both the average values, the maximum values and the seasonal variations of H_S are in good agreement with results found in previous studies of waves in the Baltic Sea (*e.g.* Tuomi *et al*, 2011 or Jönsson, *et al.* 2002).

9.3 Direction of wave propagation at desired locations

The directions of propagation are presented as cumulative bar carts, thereby illustrating how the ratios between the different directions change over the year. The charts are not primarily intended for comparison between sites, but rather to be used individually as guidance for actual work in areas adjacent to the model points. Even so, it is possible to draw some conclusions on the propagation patterns along the Swedish SE coast, and just as expected they were similar. During June to December 60-70% of the propagation is on the eastern half of the compass, with a majority going towards E or NE around the southern tip of Sweden and NE or N along the east coast. During the late winter and spring there is a shift in propagation regime with an increase in propagation towards W and S, culminating in March/April, after which the propagation directions once more turn eastward and completes the annual cycle. To further visualize this cycle a divider between waves propagating on the eastern half of the compass and on the western half has been drawn in the figures.

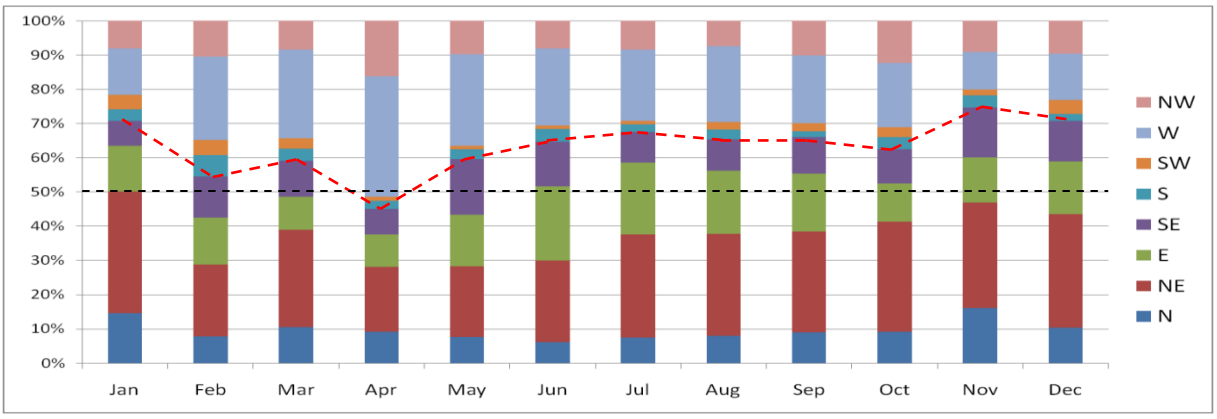

Figure 46 *Direction of propagation south of Falsterbo (direction towards which the waves are moving).*

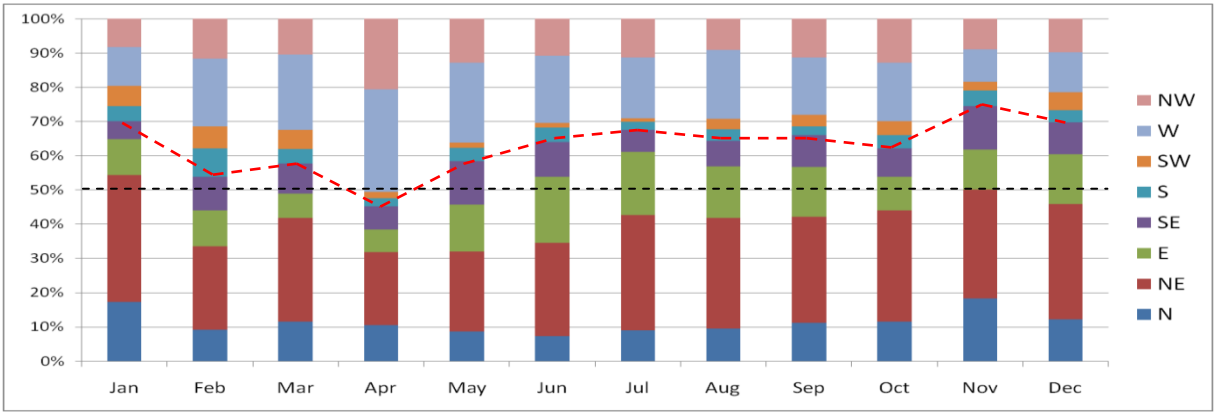

Figure 47 *Direction of propagation south of Ystad (direction towards which the waves are moving).*

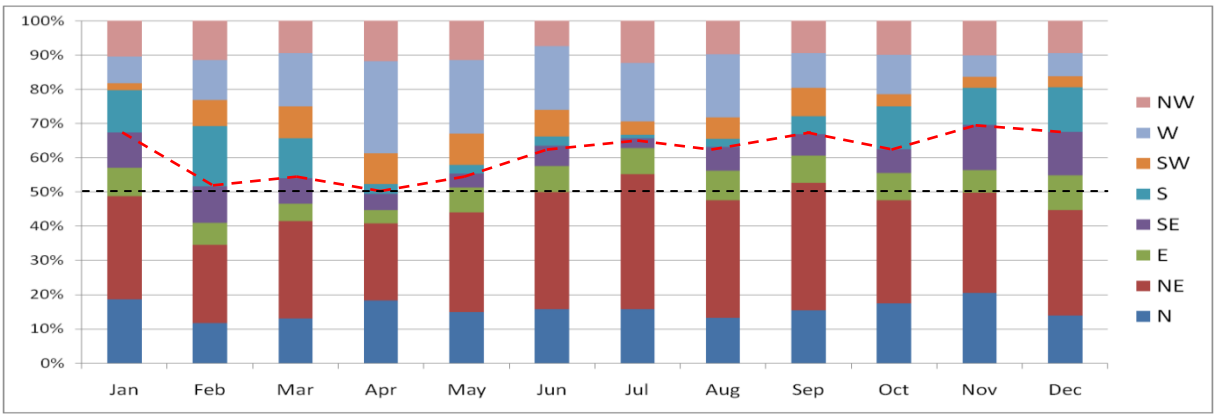

Figure 48 *Direction of propagation at Hanöbukten (direction towards which the waves are moving).*

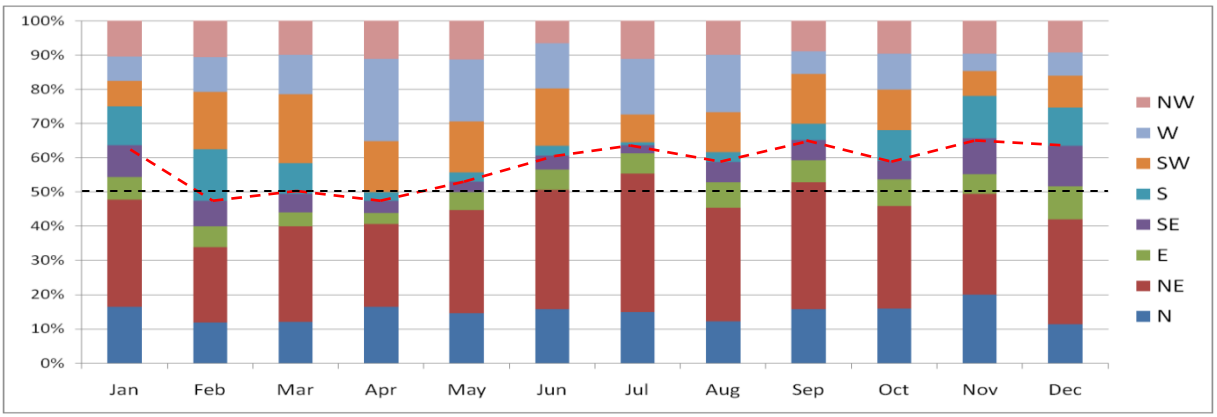

Figure 49 *Direction of propagation east of Öland (direction towards which the waves are moving).*

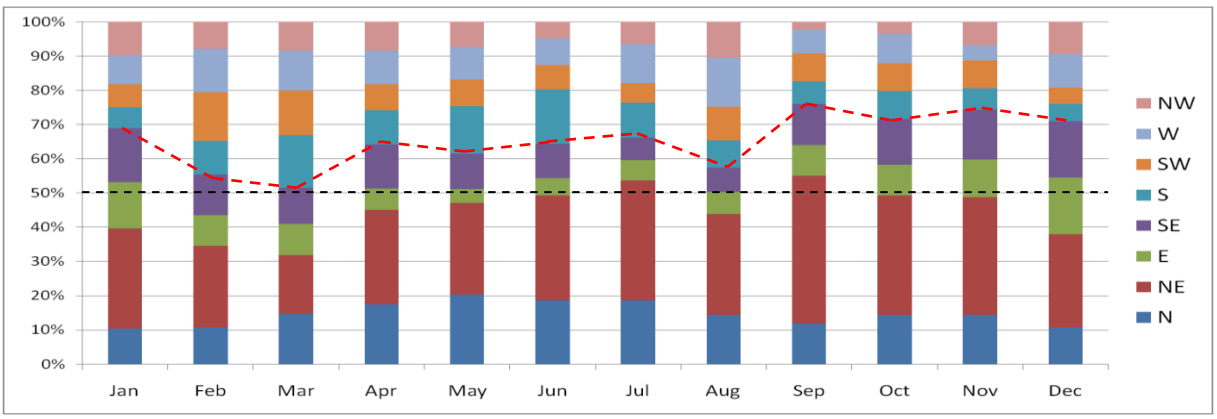

Figure 50 *Direction of propagation south of Nynäshamnm (direction towards which the waves are moving).*

9.4 Peak period

The peak periods are presented both as maximum and average values given from the model. Due to the large spread of the scatter clouds discussed in Chapter 7 and Chapter 9.1 it is not straight forward to determine the applicability of these results. The similarity in average values between the different locations and over the different months show that the average peak period varies little in space and time.

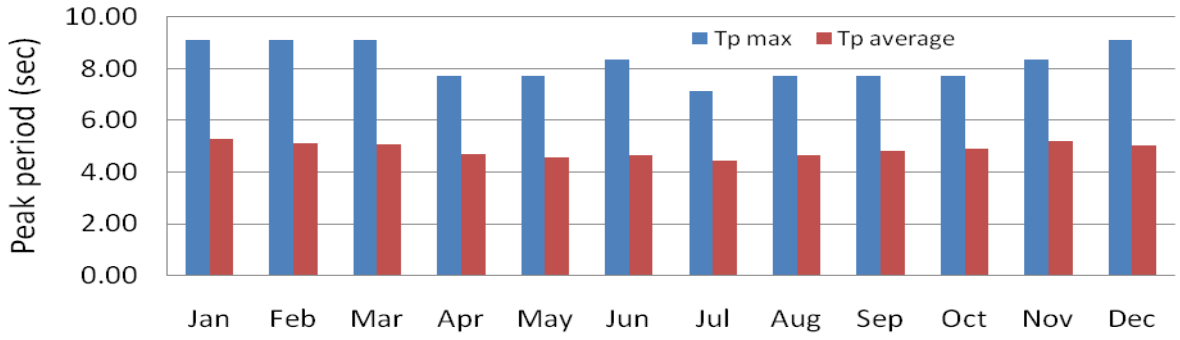

Figure 51 *Maximum and average peak periods given by the model south of Falsterbo.*

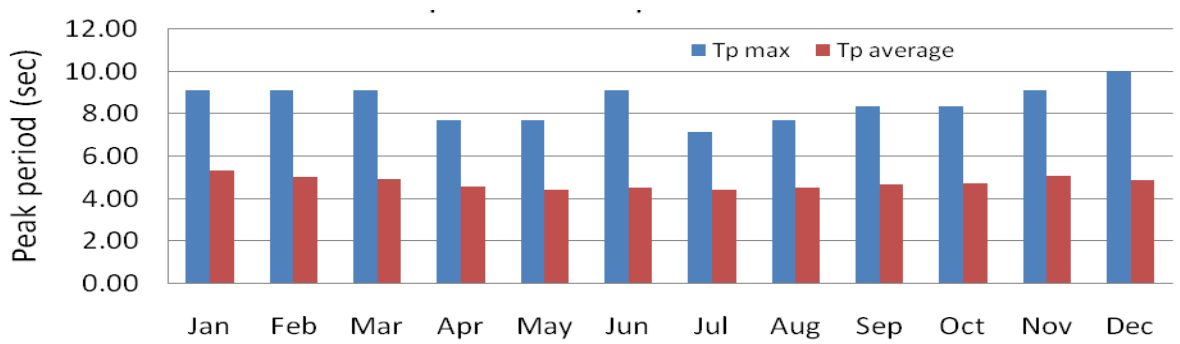

Figure 52 *Maximum and average peak periods given by the model south of Ystad.*

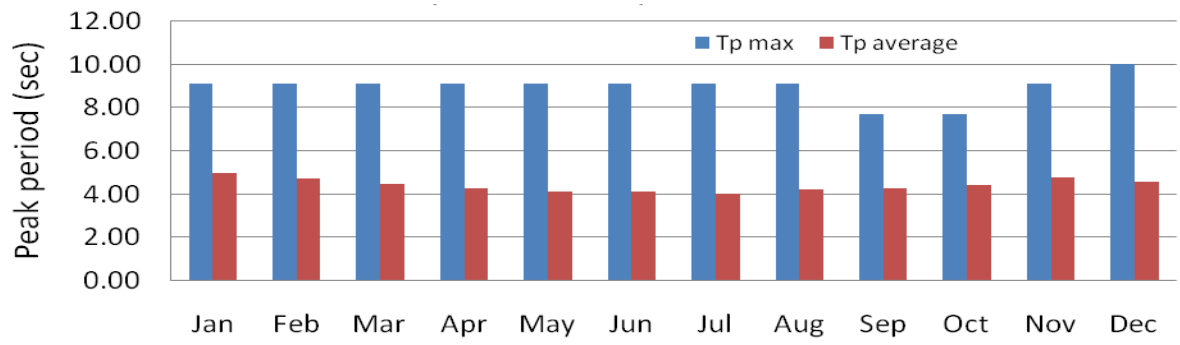

Figure 53 *Maximum and average peak periods given by the model at Hanöbukten.*

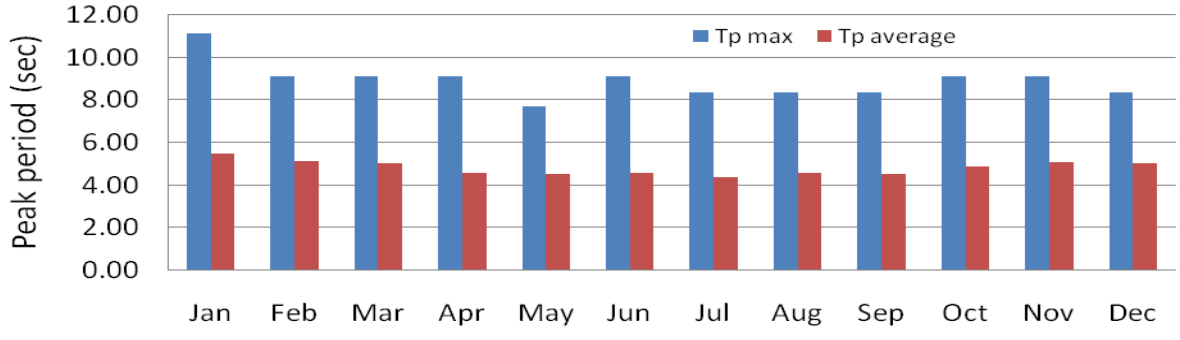

Figure 54 *Maximum and average peak periods given by the model east of Öland.*

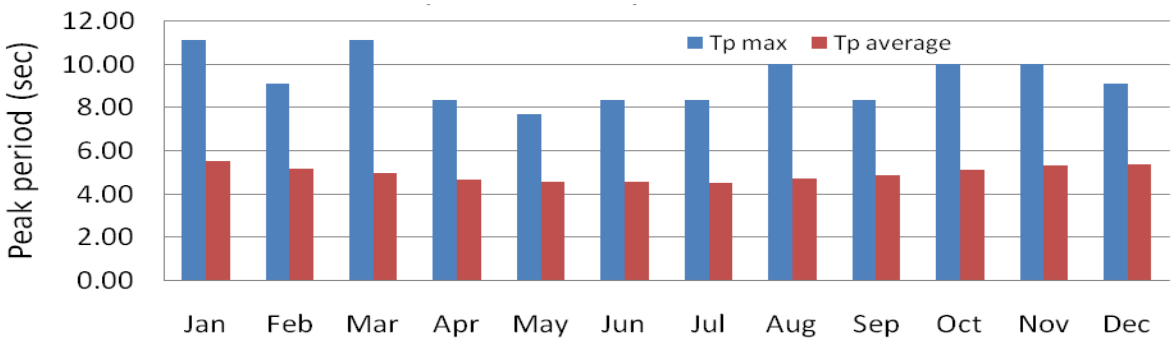

Figure 55 *Maximum and average peak periods given by the model south of Nynäshamn.*

10 Discussion

One of the greatest uncertainties of the study was the validity of using point source wind measurements to describe the wind field over the Baltic Sea, as such an approach required similar wind patterns over the entire Baltic area. The extensive analysis of the available wind measurements with respect to both direction and magnitude showed that wind patterns were indeed similar along the Baltic coasts, making the allocation of single values to larger areas highly reasonable. The effect of wind measurements being taken on land instead of over open water was also thoroughly investigated through three different wind setups deriving from both theoretical and practical experiences from earlier studies.

As for the validity of the results presented above it must be considered as high. Four different validation runs were performed to fully understand the model's response to varying circumstances, and the resulting regression lines showed that the average values of H_S and direction of propagation were represented well. This was also seen when comparing the monthly average values of model and measurements at Södra Östersjön and Huvudskär ost. Even so, the top-portion of the wave heights were consistently underestimated, so it is likely that the results for rough weather illustrated in Figure 43 are a little low. This becomes especially important when using the cumulative distribution of the waves presented in Figure 45, as the accuracy of the top-portion of the waves is crucial for the graph's applicability. The uncertainty of the higher waves means that the distribution is not accurate enough to be used for actual design, but it is still very illustrative of how the waves are distributed. When it comes to the lower end of the wave height spectra the model gave a consistent overrepresentation, probably due to the shape of the logarithmic expression used to increase the winds. Going back to Figure 17 the reader can see that at speeds of 4 m/s the wind is increased by a factor 1.5, and the factor grows rapidly as the speed approaches zero. By limiting the growth factor it is believed that most of the overrepresentation seen can be avoided, but as the lower waves are most often of little importance such actions have little impact on the waves of interest. The fact that only 6 years of data were used could be seen as a hampering condition for the proper description of the top end of the wave climate of an area, but as two very severe storms fell within the period it is not believed that high waves were missed due to the short time span.

When it comes to the maximum values of H_S they are based on single model outputs, and could hence be misleading, but a quick glance at the following 10 waves reveled that none of maxima were outliers. This, along with the fact that the values were reasonable and the that none of the scatterplotts showed any tendencies for extreme overestimation of wave heights with the chosen setup, makes it unlikely that they are the results of single model overestimations. It is on the contrary more probable that they are too low, just as the rough-weather waves.

For the direction of wave propagation the model showed minor difficulties with the timing of shifts in direction, but no real difficulties in calculating the general pattern. One possible concern to the validity of the results at the selected locations is the fact that all validation was done in deep water, where the effects of refraction were minor. The selected model points are in depths of around 10-15 m, so some refraction might have occurred. A rough assessment of the refraction effect was obtained by looking at the propagation directions at a grid cell one grid step south of each model point, where the water was deeper, and then comparing the differences between the two cells. The technique was crude and was only done for a limited amount of values, but it seemed as if the waves were turned by refraction in the expected direction. Based on this the wave directions are considered as reliable.

The greatest uncertainties of model results lay with the peak periods. Timeline plots of the modeled and measured peak periods showed how the model followed the general trend of the measurements well, especially for the chosen wind setup, so based on this there was little reason to doubt the model results. At the same time the scatterplots showed a substantial spread, but very good regression coefficients. The combined assessment of this is that the timeline plots were good enough not to doubt the average values, but that results from short or individual events cannot be trusted.

As a concluding remark the model results are believed to give reliable and solid guidelines on the wave climate at five locations along the Swedish east coast. They can be used as good and reliable estimates for a range of different applications, but as guidelines they should not be confused for exact representations of reality.

Appendices

Appendix 1

Details on the wind stations and the wave buoys available for the study.

Table 7 *List of meteorological stations in SMHI regime used for this study.*

Station name	Lat	Lon	Start of data series	End of data series
Falsterbo	55.38°	12.82°	1961-01-01 00:00	2009-12-13 21:00
Ölands södra udde	56.20°	16.40°	1961-01-01 00:00	1995-12-31 21:00
Ölands södra udde A	56.20°	16.40°	1995-01-01 00:00	2009-12-31 21:00
Hoburg	56.92°	18.15°	1961-01-01 00:00	2009-12-31 21:00
Gotska sandön	58.39°	19.20°	1961-01-01 00:00	2006-12-31 21:00
Gotska sandön A	58.39°	19.20°	1996-01-01 00:00	2009-12-31 21:00
Svenska högarna	59.44°	19.51°	1961-01-01 00:00	2009-12-31 21:00

Table 8 *List over meteorological stations in DWD regime used for this study.*

Station name	Lat	Lon	Start of data series	End of data series
Fehmarn	54.32°	11.04°	2004-01-01 00:00	2010-12-31 21:00
Arkona	54.41°	13.26°	2004-01-01 00:00	2010-12-31 21:00

Table 9 *List over meteorological stations in LEGMC regime used for this study.*

Station name	Lat	Lon	Start of data series	End of data series
Liepaja	56.48°	21.02°	2004-01-01 00:00	2009-12-31 21:00
Kolka	57.75°	22.59°	2004-01-01 00:00	2009-12-31 21:00
Pavilosta	56.89°	21.19°	2004-01-01 00:00	2004-01-01 00:00

Table 10 *List over meteorological stations in FMI regime used for this study.*

Station name	Lat	Lon	Start of data series	End of data series
Russarö	59.77°	22.95°	2004-01-01 00:00	2010-12-30 21:00
Gråhara	60.10°	24.98°	2004-01-01 00:00	2010-12-30 21:00

Table 11 *Wave buoys supplied by the SMHI.*

Wave buoy name	Lat	Lon	Measuring interval	Start of data series	End of data series
Södra Östersjön	18.47°	55.55°	1 hour	2005-01-01 00:00	2010-12-31 21:00
Huvudskär ost	19.10°	58.56°	1 hour	2001-01-01 00:00	2010-12-31 21:00
Finngrundet	18.37°	60.54°	1 hour	2006-01-01 00:00	2010-12-31 21:00
Svenska Björn	20.21°	59.28°	1 hour	1982-01-01 00:00	1986-12-31 21:00
Gustav Dahlén	17.28°	58.36°	1 hour	1983-01-01 00:00	1987-12-31 21:00
Almagrundet	19.08°	59.09°	1 hour	1978-01-01 00:00	2003-12-31 21:00

Table 12 *Wave buoys supplied by the DWD.*

Wave buoy name	Lat	Lon	Measuring interval	Start of data series	End of data series
Arkona	12.70°	54.70°	1 hour	2004-01-01 00:00	2010-12-31 21:00
Darss Sill	13.54°	54.54°	1 hour	2004-01-01 00:00	2010-12-31 21:00

Table 13 *Wave buoys available from the FMI.*

Wave buoy name	Lat	Lon	Measuring interval	Start of data series	End of data series
Northern Baltic	21.00°	59.25°	0.5 hour	2008-01-01 00:00	2009-12-31- 21:00

Appendix 2

Map of the location of the areas of influence assigned to each meteorological station. The first map shows the areas of influences when all the wind stations are included, the second map shows areas when the Latvian stations are excluded. The area over Kattegat was given a wind speed of 0 m/s, thereby not contributing with any waves but still allowing wave energy to escape.

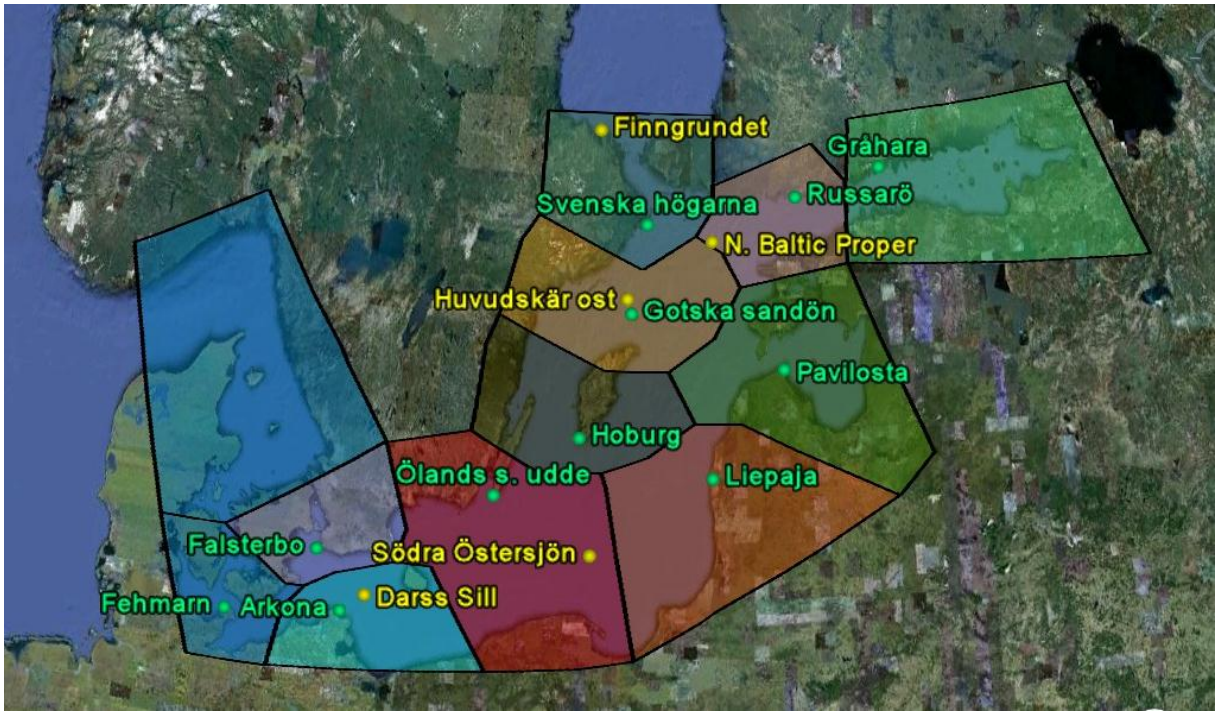

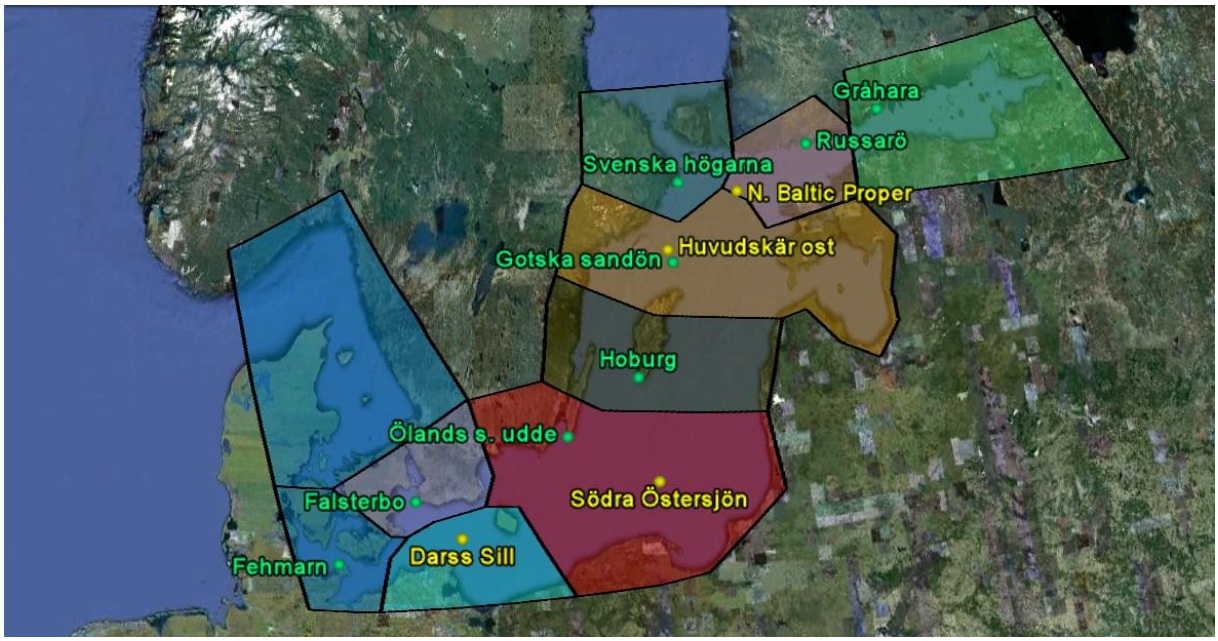

Appendix 3

Table of model wave heights and wave direction for test runs with the calculation time step 60sec and 180 sec. The table also shows the difference between the two time steps.

Table 14 *Values of H_s for equal input wind but two different calculation time steps. The first part of the table shows the actual values while the second part shows the difference between the 60 sec time step and the 180 sec time step.*

Longitude		14.02	15.42	15.42	16.62	17.42	18.22	18.82	19.62	19.82	20.62	21.02	21.62	23.02	23.62	27.22	Output
Latitude		54.31	55.71	54.91	56.11	58.11	55.11	62.71	61.51	57.71	55.31	61.51	59.51	64.71	57.51	59.91	time
Calculation time step (sec)	60	1.27	1.45	1.48	1.41	1.34	1.45	1.39	1.5	1.44	1.5	1.5	1.5	1.49	1.41	1.45	3 o'clock
	180	1.27	1.45	1.48	1.41	1.34	1.45	1.39	1.5	1.44	1.5	1.5	1.5	1.49	1.41	1.45	
	60	1.24	1.47	1.53	1.49	1.35	1.45	1.44	1.57	1.51	1.6	1.59	1.58	1.52	1.35	1.43	6 o'clock
	180	1.24	1.47	1.54	1.49	1.35	1.45	1.44	1.57	1.51	1.6	1.59	1.59	1.52	1.35	1.43	
	60	1.22	1.48	1.5	1.53	1.43	1.41	1.5	1.53	1.56	1.63	1.61	1.61	1.49	1.32	1.37	9 o'clock
	180	1.22	1.48	1.5	1.53	1.43	1.41	1.51	1.53	1.56	1.63	1.61	1.61	1.49	1.32	1.37	
	60	1.25	1.47	1.45	1.52	1.5	1.38	1.51	1.5	1.56	1.6	1.59	1.61	1.46	1.32	1.33	12 o'clock
	180	1.25	1.47	1.45	1.52	1.5	1.38	1.52	1.5	1.56	1.6	1.59	1.61	1.46	1.31	1.33	
	60	1.27	1.46	1.41	1.52	1.5	1.36	1.5	1.49	1.55	1.56	1.53	1.6	1.44	1.3	1.29	15 o'clock
	180	1.27	1.46	1.4	1.52	1.5	1.35	1.5	1.49	1.55	1.56	1.53	1.6	1.44	1.3	1.29	
	60	1.26	1.47	1.38	1.52	1.47	1.36	1.52	1.49	1.57	1.5	1.48	1.6	1.42	1.27	1.28	18 o'clock
	180	1.26	1.47	1.38	1.52	1.47	1.36	1.52	1.49	1.57	1.5	1.47	1.6	1.42	1.27	1.28	
	60	1.29	1.49	1.38	1.53	1.49	1.37	1.55	1.5	1.58	1.39	1.42	1.6	1.4	1.25	1.27	21 o'clock
	180	1.29	1.49	1.38	1.53	1.49	1.37	1.54	1.49	1.58	1.39	1.42	1.6	1.39	1.25	1.26	
	60	1.36	1.5	1.41	1.52	1.53	1.4	1.55	1.5	1.58	1.29	1.35	1.56	1.35	1.21	1.22	24 o'clock
	180	1.36	1.49	1.4	1.51	1.53	1.39	1.55	1.5	1.58	1.28	1.34	1.56	1.35	1.2	1.21	
Resulting differences for the two different time steps																	
Δ(60-180)		0	0	0	0	0	0	0	0	0	0	0	0	0	0	0	3 o'clock
Δ(60-180)		0	0	-0.01	0	0	0	0	0	0	0	0	-0.01	0	0	0	6 o'clock
Δ(60-180)		0	0	0	0	0	0	-0.01	0	0	0	0	0	0	0	0	9 o'clock
Δ(60-180)		0	0	0	0	0	0	-0.01	0	0	0	0	0	0	0.01	0	12 o'clock
Δ(60-180)		0	0	0.01	0	0	0.01	0	0	0	0	0	0	0	0	0	15 o'clock
Δ(60-180)		0	0	0	0	0	0	0	0	0	0	0.01	0	0	0	0	18 o'clock
Δ(60-180)		0	0	0	0	0	0	0.01	0.01	0	0	0	0	0.01	0	0.01	21 o'clock
Δ(60-180)		0	0.01	0.01	0.01	0	0.01	0	0	0	0.01	0.01	0	0	0.01	0.01	24 o'clock

Appendix 4

Comparison of H_s and wave directions at buoy locations when including a) only southern Baltic or b) the entire Baltic

Table 15 *Resulting H_s and wave direction when both including and excluding the Sea of Bothnia. The reason for Finngrundet being 0 in the southern run is that this buoy is in the northern half of the Baltic.*

Souther Baltic only												
	Significant wave height						Mean wave direction					
	Dras Sill	Arkona	Södra Östersjön	Northern Baltic	Finngrundet	Huvudskär Ost	Dras Sill	Arkona	Södra Östersjön	Northern Baltic	Finngrundet	Huvudskär Ost
2010-04-09 03	1.08	1.28	1.5	1.49	0	1.47	78	68	75	74	0	76
2010-04-09 06	1.03	1.26	1.54	1.55	0	1.48	55	53	65	59	0	64
2010-04-09 09	0.97	1.19	1.5	1.57	0	1.39	28	36	51	43	0	50
2010-04-09 12	0.99	1.15	1.47	1.57	0	1.3	360	15	29	26	0	27
2010-04-09 15	1.07	1.13	1.48	1.58	0	1.28	332	350	1	9	0	357
2010-04-09 18	1.18	1.14	1.45	1.58	0	1.3	312	323	336	349	0	329
2010-04-09 21	1.23	1.22	1.42	1.59	0	1.36	294	295	313	327	0	305
2010-04-10 00	1.28	1.31	1.44	1.58	0	1.43	275	274	290	303	0	286
Entire Baltic												
	Significant wave height						Mean wave direction					
	Dras Sill	Arkona	Södra Östersjön	Northern Baltic	Finngrundet	Huvudskär Ost	Dras Sill	Arkona	Södra Östersjön	Northern Baltic	Finngrundet	Huvudskär Ost
2010-04-09 03	1.08	1.28	1.5	1.49	1.14	1.47	78	68	75	74	81	76
2010-04-09 06	1.03	1.26	1.54	1.55	1.05	1.48	55	53	65	59	59	64
2010-04-09 09	0.97	1.19	1.5	1.57	0.96	1.39	28	36	51	43	33	50
2010-04-09 12	0.99	1.15	1.47	1.57	0.96	1.3	360	15	29	26	6	27
2010-04-09 15	1.07	1.13	1.48	1.58	0.99	1.28	332	350	1	9	337	357
2010-04-09 18	1.18	1.14	1.45	1.58	1.09	1.3	312	323	336	349	310	329
2010-04-09 21	1.23	1.22	1.42	1.59	1.17	1.36	294	295	313	327	291	305
2010-04-10 00	1.28	1.31	1.44	1.58	1.25	1.43	275	274	290	303	273	286
Difference between having only southern Baltic and the entire Baltic												
2010-04-09 03	0	0	0	0	-1.14	0	0	0	0	0	-81	0
2010-04-09 06	0	0	0	0	-1.05	0	0	0	0	0	-59	0
2010-04-09 09	0	0	0	0	-0.96	0	0	0	0	0	-33	0
2010-04-09 12	0	0	0	0	-0.96	0	0	0	0	0	-6	0
2010-04-09 15	0	0	0	0	-0.99	0	0	0	0	0	-337	0
2010-04-09 18	0	0	0	0	-1.09	0	0	0	0	0	-310	0
2010-04-09 21	0	0	0	0	-1.17	0	0	0	0	0	-291	0
2010-04-10 00	0	0	0	0	-1.25	0	0	0	0	0	-273	0

Appendix 5

Direction of wave propagation at Södra Östersjön and Huvudskär ost during 2007. To make the graphs clearer only the periods where measurements were available were included.

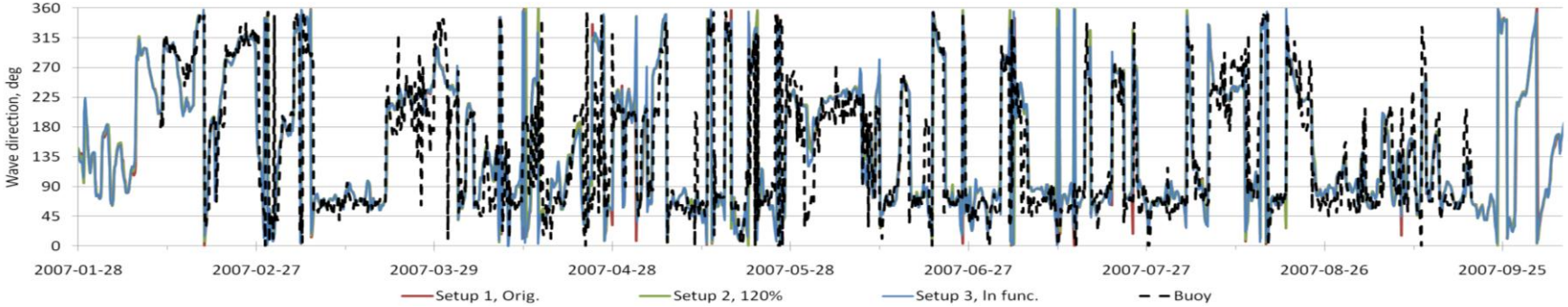

Figure 56 *Wave direction Södra Östersjön.*

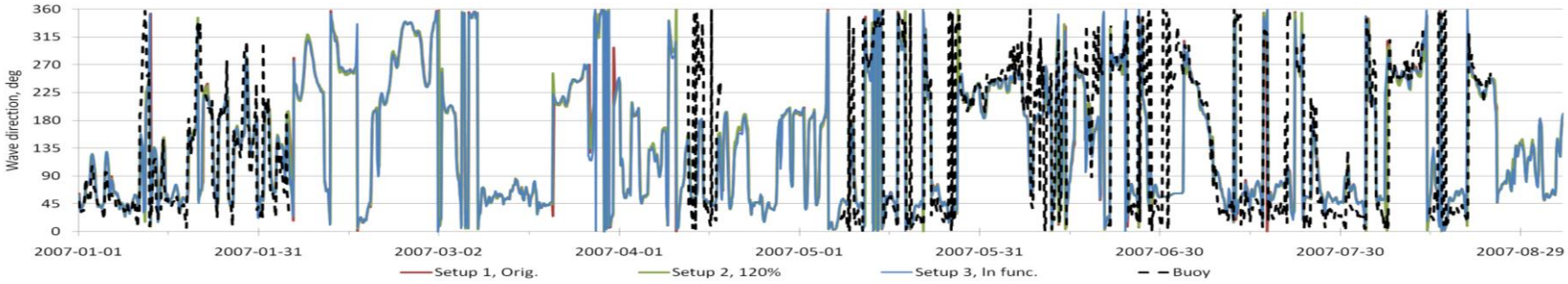

Figure 57 *Wave direction Huvudskär ost.*

Wave peak periods at Södra Östersjön and Huvudskär ost during 2007. To make the graphs more readable only the periods in which there were buoy measurements are presented.

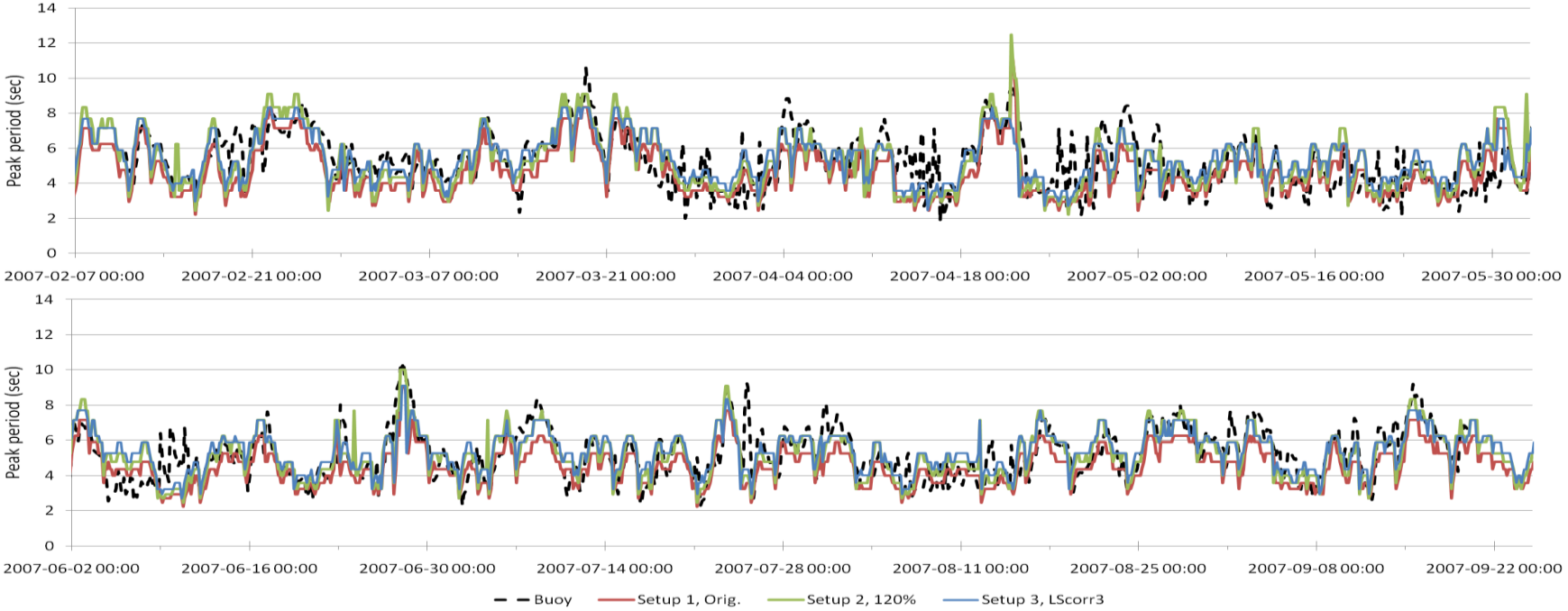

Figure 58 *Peak period at Södra Östersjön. The figure has been cut into two to make it more readable.*

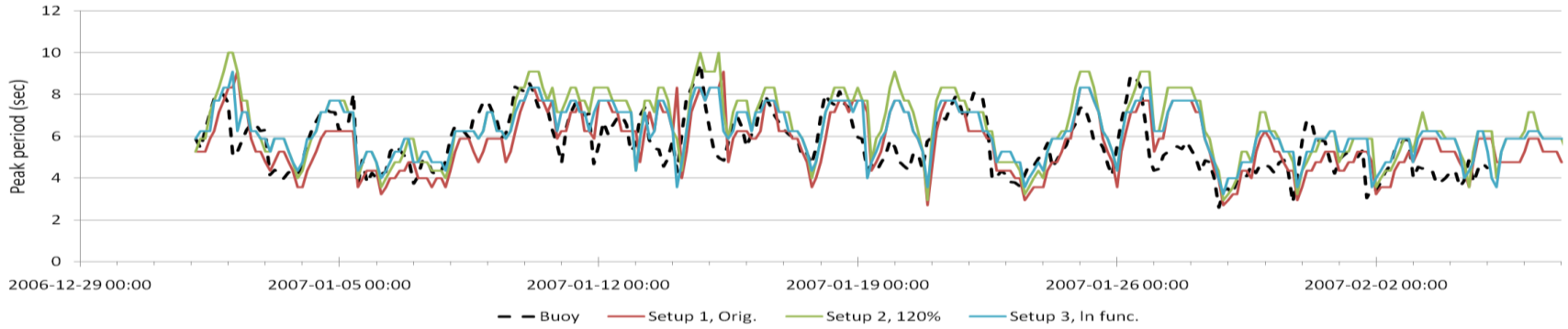

Figure 59 *Peak period at Huvudskär ost.*

Appendix 6

Tables of correlation coefficients and R^2 values for H_s for all the validation runs

Table 16 *Regression coefficients and R^2 values on H_s for the 2007 validation run. Note how Setup 2 and 3 give similar regression coefficients, but Setup 2 gives a better R^2 value due to internal distortion of Setup 3.*

		Forced linear regression			Free linear regression		
		Setup 1	Setup 2	Setup 3	Setup 1	Setup 2	Setup 3
Darss Sill	Reg. coeff	0.78	1.04	0.94	0.68	0.93	0.69
	R^2 value	0.73	0.74	0.61	0.76	0.76	0.77
Södra Östersjön	Reg. coeff	0.68	0.95	0.93	0.55	0.77	0.64
	R^2 value	0.61	0.64	0.44	0.68	0.65	0.62
Huvudskär ost	Reg. coeff	0.68	0.94	0.93	0.53	0.78	0.64
	R^2 value	0.49	0.55	0.46	0.56	0.58	0.68

Table 17 *Regression coefficients and R^2 values on H_s for the October 2009 validation run.*

		Forced linear regression			Free linear regression		
		Setup 1	Setup 2	Setup 3	Setup 1	Setup 2	Setup 3
Darss Sill	Reg. coeff	0.57	0.74	0.83	0.50	0.72	0.69
	R^2 value	0.38	0.40	0.41	0.60	0.67	0.43
Södra Östersjön	Reg. coeff	0.67	0.90	1.00	0.38	0.62	0.55
	R^2 value	0.21	0.51	0.13	0.60	0.67	0.59
Huvudskär ost	Reg. coeff	0.80	1.08	1.13	0.64	0.93	0.82
	R^2 value	0.63	0.64	0.55	0.68	0.66	0.66

Table 18 *Regression coefficients and R^2 values on H_s for the January 2005 validation run (storm Gudrun).*

		Forced linear regression			Free linear regression		
		Setup 1	Setup 2	Setup 3	Setup 1	Setup 2	Setup 3
Darss Sill	Reg. coeff	0.75	0.99	0.83	0.69	0.91	0.65
	R^2 value	0.82	0.81	0.74	0.83	0.82	0.83

Table 19 *Regression coefficients and R^2 values on H_s for the January 2007 validation run (storm Pär).*

		Forced linear regression			Free linear regression		
		Setup 1	Setup 2	Setup 3	Setup 1	Setup 2	Setup 3
Darss Sill	Reg. coeff	0.69	0.92	0.78	0.76	1.00	0.76
	R^2 value	0.75	0.76	0.68	0.76	0.77	0.74
Huvudskär ost	Reg. coeff	0.73	1.08	0.98	0.62	1.01	0.75
	R^2 value	0.35	0.46	0.48	0.37	0.47	0.54

References

Publications

Berg, C. (n.d.). *Validation of the WAM model over the Baltic Sea*. Masters thesis project at the University of Upsala.

Blomgren, S., Larson, M., Hanson, H., 1999, *Numerical modelling of the wave climate in the Southern Baltic Sea*, Journal of coastal research.

CEM, 2006. *Coastal Engineering Manual*.

Jensen, R., 1994, *Spectral wave modelling technology*. Costal Engineering Technical Note 9.

Jönsson, A., Broman, B., Rahm, l., 2002, *Variation in the Baltic Sea wave field*¸ Ocean Engineering 30 (pp 107-126).

Komen, G.J., Cavaleri, L., Dinelan, M., Hasselmann, K., Hasselmann, S., Jansen, P.A.E.M., 1994, *Dynamics and Modelling of Ocean Waves*, Cambridge, Press Syndicate of the University of Cambridge.

Moore, D. S., 1997, *Statistics - Concepts and controversies*, New York, W.H. Freeman and Co.

Sverdrup, H.U., Munk, W., 1947, *Wind, sea and swell - theory of relations for forcasting*, Washington D.C, U.S. Navy Hydrographical Office.

Rosman, P., 2007, *Modelos para recursos hídricos*. Rio de Janeiro: COOPE.

SMHI. (2010). *Vågor i svenska hav - Faktablad 46*. Swedish Meteorological and Hydrological Institute.

SPM. (1984). *Shore Protection Manual* (pp. 3-30). Washington: US Army Corp of Engineers.

Tuomi, L, Kahma, K.K., Pettersson, H., 2011, *Wave hindcast statistic in seasonally ice-covered Baltic Sea*, Finnish Meteorological Institute, Helsinki

Vännman, K. (2002). *Matematisk statestisk*. Lund: Studentlitteratur.

Electronic sources

SMHI. (2009a). *Isförhållanden i Östersjön*, Retrieved 2011-05-10, from Swedish Meteorological and Hydrological Institute webpage: http://www.smhi.se/kunskapsbanken/oceanografi/ostersjons-och-vasterhavets-geografi-1.3080

SMHI. (2009b). *Isförhållanden i Östersjön*, Retrieved 2011-05-10, from Swedish Meteorological and Hydrological Institute webpage: http://www.smhi.se/kunskapsbanken/oceanografi/isforhallanden-i-ostersjon-1.7024

SMHI. (2009c). *Gudrun – Januaristormen 2005*, Retrieved 2011-04-17 from Swedish Meteorological and Hydrological Institute webpage: http://www.smhi.se/kunskapsbanken/meteorologi/gudrun-januaristormen-2005-1.5300

Östersjöportalen, (2009), *Östersjöns form, areal och volym*, Retrieved 2011-04-17 from Östersjöportalen webpage: http://www.itameriportaali.fi/sv/tietoa/yleiskuvaus/sv_SE/muoto_ala_tilavuus/

Interviews

Bertotti, L. of the Institute of Marine Science (ISMAR) in Venice, 2011-04-10.